NRC Research Press

REVIEW

Evolution, history, and use of stem taper equations: a review of their development, application, and implementation[1]

John Paul McTague and Aaron Weiskittel

Abstract: Stem taper equations, which predict the change in stem form from ground to tip, have become the primary means for estimating bole volume. Stem taper equations can provide predictions with similar levels of accuracy as volume equations, but with greater flexibility, a wider range of potential uses, and consistency between taper and volume. This review is a synthesis of the current state of knowledge on stem taper equations and an assessment of challenges for future model refinement. It includes the history and evolution of stem taper model forms, which have received tremendous attention and focus over the last several decades. Additional focal areas covered are (*i*) the use of additional covariates beyond tree diameter at breast height (DBH) and total height; (*ii*) alternative statistical methods for developing stem taper equations such as parametric, semiparametric, and nonparametric approaches; (*iii*) key considerations for proper development, application, and use of stem taper equations such as sample size requirements, local calibration, and evaluation; and (*iv*) a synthesis of key findings, future opportunities, and ongoing challenges. Current and developing technologies such as terrestrial laser scanning (TLS) offer an unprecedented opportunity to measure stem form in much greater detail at significantly lower costs and time requirements than traditional methods. Overall, continued development, refinement, and application of stem taper equations will remain important given the critical nature of tree volume for science, accurate inventories, and ultimately, sustainable forest management.

Key words: bole volume, stem form, forest inventory, parametric, semiparametric, nonparametric, regression.

Résumé : Les équations de défilement des tiges, qui prédisent les changements dans la forme des tiges du sol jusqu'à l'extrémité, sont devenues le principal moyen pour estimer le volume du tronc. Les équations de défilement des tiges peuvent fournir des prédictions avec des niveaux de précision semblables aux équations de volume, mais avec une plus grande flexibilité, un éventail d'usages potentiels plus grand et une cohérence entre le défilement et le volume. Cet article est une synthèse de l'état actuel des connaissances sur les équations de défilement et une évaluation des défis à surmonter pour raffiner les futurs modèles. Cela inclut l'historique et l'évolution des formes de modèles de défilement, qui a suscité beaucoup d'intérêt et reçu beaucoup d'attention au cours des quelques dernières décennies. Les zones additionnelles d'intérêt couvertes sont (*i*) l'utilisation de covariables additionnelles autres que le diamètre des arbres à hauteur de poitrine (dhp) et la hauteur totale; (*ii*) les méthodes statistiques alternatives pour élaborer des équations de défilement des tiges telles que les approches paramétriques, semi-paramétriques et non paramétriques; (*iii*) les princ ipales considérations pour le développement, l'application et l'utilisation appropriés des équations de défilement des tiges telles que les exigences concernant la taille de l'échantillon, la calibration locale et l'évaluation; et (*iv*) une synthèse des principales constatations, des opportunités futures et des défis actuels. Les technologies courantes et en voie de développement, telles que le balayage laser terrestre, offrent des opportunités sans précédents de mesurer la forme des tiges de façon beaucoup plus détaillée à des coûts significativement plus faibles et beaucoup plus rapidement que les méthodes traditionnelles. Globalement, l'application, le raffinement et le développement continu des équations de défilement des tiges vont demeurer importants étant donné le caractère crucial du volume des arbres pour la science, la précision des inventaires et ultimement l'aménagement forestier durable. [Traduit par la Rédaction]

Mots-clés : volume du tronc, forme de la tige, inventaire forestier, paramétrique, semi-paramétrique, non paramétrique, régression.

1. Introduction

Tree volume, particularly merchantable volume, is a primary attribute that strongly influences forest management and planning. However, tree volume is difficult to measure and assess directly because of time and effort involved, the general requirement to destructively sample, and the complex nature of stem form, which generally requires water displacement technique or xylometry for true accuracy (Filho and Schaaf 1999). Consequently, tree volume estimation often relies on the application of empirically derived volume or taper equations. Because of their level of accuracy and high flexibility, stem taper equations have become a standard method for estimating tree volume in

Received 7 July 2020. Accepted 28 September 2020.

J.P. McTague. Southern Cross Biometrics, 95172 Bermuda Dr., Fernandina Beach, FL 32034, USA.
A. Weiskittel.* Center for Research on Sustainable Forests, University of Maine, Orono, ME 04469-5755, USA.
Corresponding author: Aaron Weiskittel (email: aaron.weiskittel@maine.edu).
*Aaron Weiskittel currently serves as an Associate Editor; peer review and editorial decisions regarding this manuscript were handled by Thomas Nord-Larsen.
[1]This review is part of the special issue "Historical perspectives in forest sciences", which celebrates the 50th anniversary of the *Canadian Journal of Forest Research*.

recent decades. Stem taper equations have been discussed in detail in various forestry textbook chapters (Weiskittel et al. 2011; Burkhart and Tomé 2012; Kershaw et al. 2016). Although these chapters address stem taper equations and their application in some detail, the full extent of the available and current literature has yet to be synthesized. Consequently, a comprehensive review of their primary literature and a discussion of the evolution and use of taper equations from both a scientific and practical perspective are warranted.

Stem taper equations predict the absolute or relative rate of change in the tree stem profile in either diameter inside or outside bark. Many model forms and potential predictors have been used in stem taper equations, and multiple statistical approaches and considerations for appropriate application are also worth highlighting. Consequently, this review is divided into three primary sections: (*i*) the history and evolution of stem taper model form and predictors; (*ii*) alternative statistical approaches for stem taper model parameterization; and (*iii*) considerations for effective development, application, and use of stem taper equations. The review concludes with a brief discussion on the current limitations of stem taper equations and their potential future development and application. Although stem equations are used throughout the world, greater detail in this review is focused on North America.

2. History and evolution of stem taper model form and predictors

Stem taper equations predict the change in stem profile from the ground to tree tip. Trees can be considered as a combination of geometric shapes (e.g., cylindrical, parabolic, and conical) that vary with species, tree age, and stand conditions. Goodwin (2009) noted several key criteria for a taper equation, including (*i*) high accuracy; (*ii*) reliance on predictors that are easy to obtain; (*iii*) algebraically integrable and invertible; (*iv*) continuous yet constrained to ensure that predictions are consistent with inputs; (*v*) single and nonsegmented equation; (*vi*) easily localized and able to explain the variability between trees, yet regionally applicable; (*vii*) logical behavior (e.g., stem diameter > 0, $= 0$ at total height, and = tree diameter at 1.3 m); (*viii*) integration yields total stem volume; (*ix*) invertible (e.g., $d = \tau(h) \rightarrow h = \tau^{-1}(d)$); and (*x*) applicable to a wide range of species, stand conditions, and tree sizes. Given the high variation in stem form, a wide variety of model forms and predictors have been used even for certain species and regions (Hann 1994), further highlighted in the following sections. A brief synopsis of early efforts to predict tree taper is followed by a greater focus on model forms used today.

2.1. Early efforts in predicting tree taper based on center of gravity within the crown

Dating back to the late 1800s, early predictive models for stem taper did not contain fitted coefficients, but rather relied on the theory of stem form and taper that were inferred from conjectures about the mechanical strength properties of tree stems. As summarized by Anuchin (1960) regarding the theories of Metzger (1893): "If the stem is regarded as a beam of uniform strength, the cubed diameters of any of its sections must be equal to the distance from those diameters to the crown's center of gravity". In a review of tree stem form and development, Larson (1963) stated that Metzger (1893) considered both the vertical force of the stem itself and the horizontal force imposed on the tree by wind. Anuchin (1960) stated that horizontal wind force had a bearing on the stem taper within the crown of the tree. Figure 1 provides an illustrative interpretation of stem taper below the crown's center of gravity; however, it appears based on the premise of a triangular crown shape. Below the base of the live crown, upper-stem diameter is predicted as

Fig. 1. The d^3 rule of Metzger (1893) for upper-stem diameters below the live crown, whereby the diameters cubed are proportional to length: $d_1^3 : d_2^3 : d_3^3 = l_1 : l_2 : l_3$. Figure from Anuchin (1960).

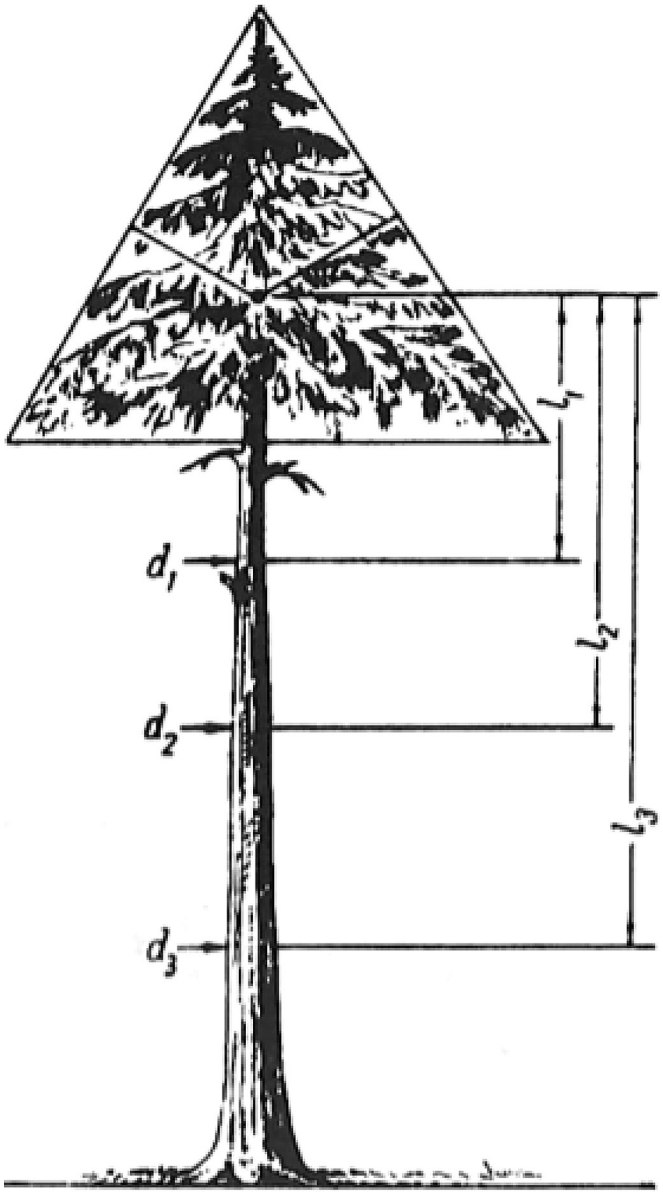

$$d_u = d_{cb}\left(\frac{cl + 3 \times dist_{cb}}{cl}\right)^{1/3} \quad (1)$$

where d_u is upper-stem diameter in centimetres, d_{cb} is upper-stem diameter at the crown base in centimetres, cl is crown length in metres, and $dist_{cb}$ is distance in metres from d_u to d_{cb}.

Within the crown, the stem is assumed to have conic taper, and upper-stem diameter is computed as

$$d_u = d_{cb}\left(\frac{dist_{tip}}{cl}\right) \quad (2)$$

where $dist_{tip}$ is distance in metres from total height to the upper-stem diameter d_u.

Fig. 2. Form point is defined as the center of gravity of the crown in percentage of total height. It is measured in the field by holding a ruler, divided in tens, and aligning the sight of the top of the ruler with total tree height and the bottom of the ruler with ground-line diameter of the tree. Figure from Fogelberg (1953).

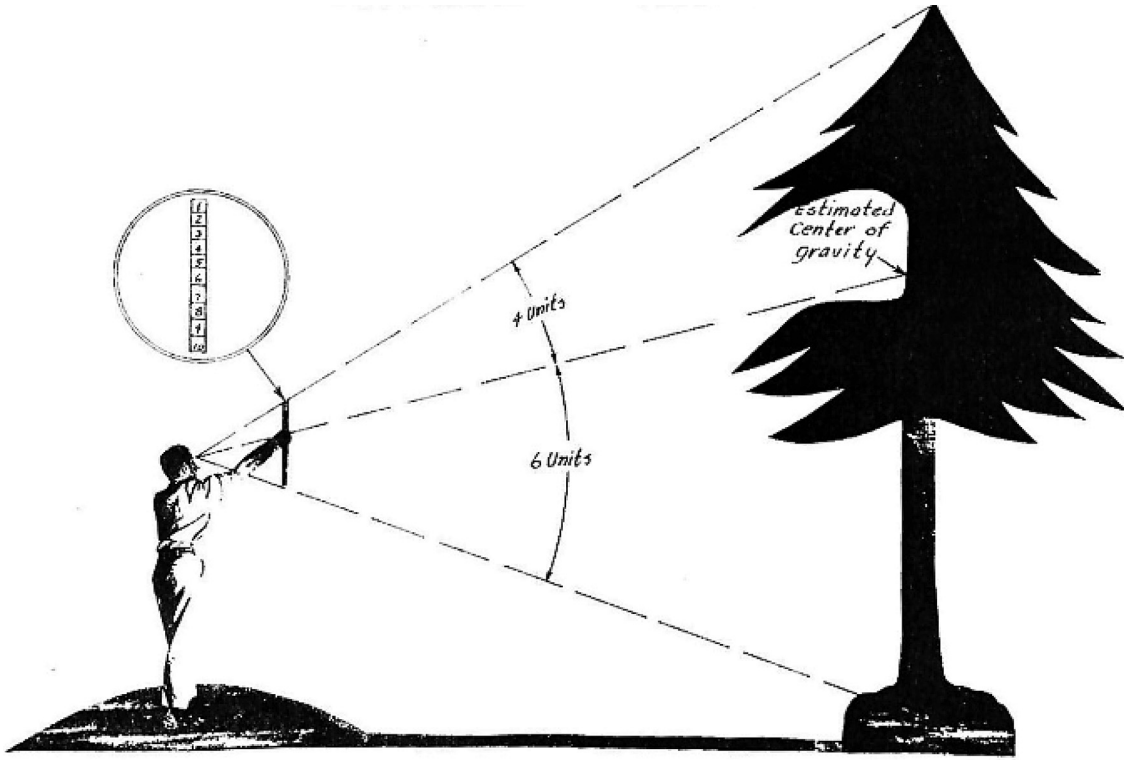

Larson (1963) referred to eq. 1 as the "d^3 rule" that follows the hypothesis of a tree stem conforming to a beam of uniform resistance to bending. Referring to Fig. 1, the cubes of upper-stem diameters are stated to be proportional to the log lengths from the crown's center of gravity: $d_1^3 : d_2^3 : d_3^3 = l_1 : l_2 : l_3$. One consideration on this hypothesis is whether the stem bole contained heartwood or not. Trees with heartwood, or a hollow uniform strength beam, were stated to have the following proportionality by Kozitsin (1909): $d_1^{4.5} : d_2^{4.5} : d_3^{4.5} = l_1 : l_2 : l_3$.

Metzger's (1893) hypothesis certainly provoked vigorous debate, with much of it centered on whether he had fully considered the effect of horizontal wind pressure. Hohenadl (1924) suggested that the diameter at any point on the stem was governed by the weight that had to be supported at that point, and Gray (1956) asserted that Metzger's hypothesized tree bole resembled a cubic paraboloid and was unnecessarily strong from a mechanical point of view. Instead, Gray advocated that the dimensions of the main stem conformed to those of a quadratic paraboloid. Regardless, the influence of Metzger and the importance of the center of gravity in determining stem form continued to have a strong role in forest measurement practices in the southern United States (US) until the early 2000s. For example, a large forest products firm in the southern US used a three-coefficient Hojer (1903) taper model (eq. 3) without any fitted parameters in its volume estimation procedures:

$$\frac{d_u}{\mathrm{DBH}} = b_0 \times \ln\left[\frac{b_1 + \left(\frac{H - h_u}{H - 1.3}\right)}{b_2}\right] \quad (3)$$

where h_u is upper-stem height in metres corresponding to upper-stem diameter d_u, H is total tree height in metres, DBH is diameter at breast height (1.3 m) in centimetres, and b_i are coefficients of the Hojer (1903) taper model. Three conditions were imposed on the taper model, thus reducing the number of free-fitted parameters to zero:

Condition	Resulting expression
when $h_u = H$, $d_u = 0$	$\ln b_2 = b_0 \times \ln b_1$
when $h_u = 1.3$, $d_u = \mathrm{DBH}$	$b_0 = \frac{1}{\ln[(b_1+1)/b_1]}$
when $h_u = \frac{H+1.3}{2}$, $\frac{d_u}{\mathrm{DBH}} = \mathrm{afc}$	$\mathrm{afc} = \frac{\ln[1+(\beta/2)]}{\ln(1+\beta)}$

where $\beta = 1/b_1$ and afc is the absolute form class (an inside-bark ratio) of upper-stem diameter to DBH at 50% of the height between 1.3 m and total height. β is solved iteratively for each tree, and it is a function of the absolute form factor. Fogelberg (1953) suggested that the tedious determination of absolute form class could be supplanted with the measurement of form point (FP), which is defined as the location above ground of the center of gravity of the crown in percentage of total height (Fig. 2). Fogelberg (1953) asserted that form point was a convenient and reliable methodology for predicting absolute form class. A simple linear function is used to predict absolute form class: afc = (32.3 + 0.515 × FP)/100.

In summary, a single coefficient for the Hojer (1903) taper model, β, is indirectly computed from an observed estimate of the tree's center of gravity. The Hojer taper model is then integrated to compute cubic volume. One troubling feature among the illustrations provided by Anuchin (1960), Gray (1956), and Fogelberg (1953) is the lack of consistency regarding the location of the center of gravity, or center of pressure on the crown. Given the difference in crown shapes, their approximation of the center of gravity certainly appears plausible, but a question arises over the repeatability of their predictions among different field observers.

Fig. 3. Geometrical solids with increasing values of r. The integrated stem profile results in volume $= \frac{1}{r+1}$(base × height), where base is the cross-sectional area at 1.3 m. Figure from Bitterlich (1984).

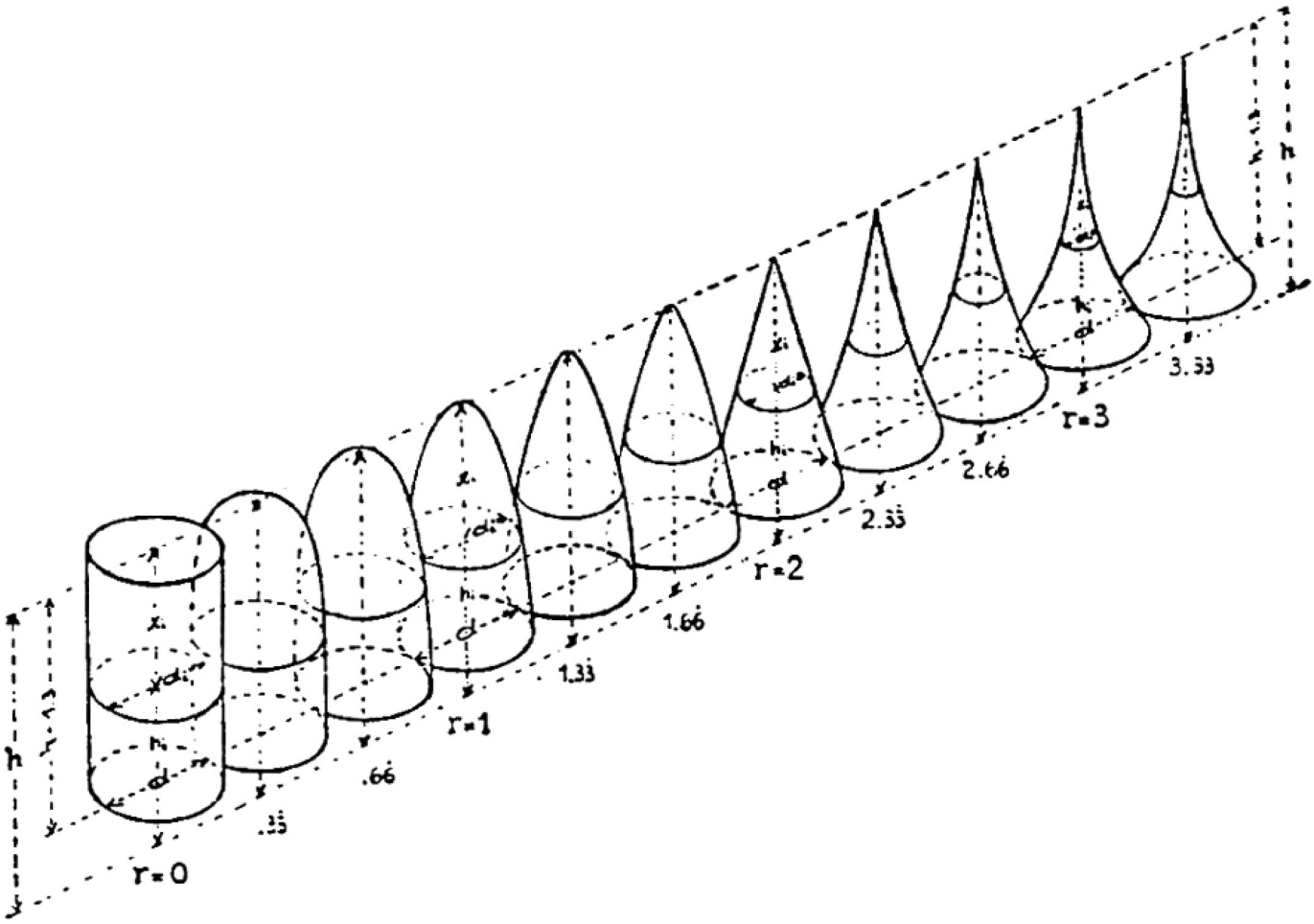

2.2. Solids of revolution

Solids of revolution represent a useful construct and introduction to stem form and taper. Although small differences exist among authors on the treatment of the left-hand side of the taper expression, Bitterlich (1984) defined a stem profile equation that is mathematically consistent with the $Y = K\sqrt{X^r}$ or $Y^2 = K \times X^r$ expression used in the standard forest mensuration textbook (e.g., Kershaw et al. 2016):

$$(4) \qquad \left(\frac{d_u}{\mathrm{DBH}}\right)^2 = \left(\frac{H - h_u}{H - 1.3}\right)^r$$

where the r exponent defines form. As demonstrated in Fig. 3, the exponent r dictates both shape and volume of the solid. When estimating standing tree volume of excurrent form, attention is generally focused on stems with the form ranging from a paraboloid ($r = 1$) to a cone ($r = 2$). Rarely does an entire tree stem resemble a neiloid ($r = 3$), and this shape is normally reserved for the bottom segment of the stem bole. Integrating the d_u^2 term of eq. 4 from 1.3 m to total height (H) provides an expression of volume above breast height (v_{bh}):

$$(5) \qquad v_{bh} = k\int_{h_u=1.3}^{h_u=H} d_u^2 \, dh_u = \frac{1}{r+1} k \times \mathrm{DBH}^2 (H - 1.3)$$

where $k = \pi/40\,000$. Using an expedient assumption that a stem bole resembles a cylinder below breast height, the total volume (v) of a tree from ground line to total height can be expressed as

$$(6) \qquad v = \frac{1}{r+1} \times g \times (H - 1.3) + g \times 1.3$$

where g is individual-tree basal area. The cylindrical form factor (ff), or $v/(g \times H)$, is then computed from either $\frac{1}{r+1}$ for volume above breast height or $\frac{1 + (1.3r/H)}{r+1}$ for total volume. Knowledge of the exponent r or form factor for a species of interest can be useful for performing quick mental computations when conducting a field reconnaissance; however, the use of eq. 4 is rarely satisfying when merchandizing a stem into multiple products. Bruce and Schumacher (1942) recognized the peril of using an erroneous assignment of geometric shape to the stem and suggested the computation of tree stem volume by graphing the stem profile and then using a planimeter to compute area and volume. This reticence to assign a tree to a solid of revolution form may partially explain why use of the Mesavage (1947) cubic-foot volume tables still lingers in the southern US. The Mesavage tables require the user to provide an estimate of form class ((d_u inside bark at 5.3 m/DBH) × 100). Mesavage (1947) provides an estimate of taper at the midpoint of the first 4.9 m log by DBH and form class. Cubic volume inside bark is then computed for the first 4.9 m log using the Huber volume formula ($v = L \times g_m$, where L is

Table 1. Overview of the primary parametric stem taper model forms with advantages, disadvantages, and examples identified.

Model form	Advantages	Disadvantages	Example(s)
Variable-form	Highly flexible with robust performance across multiple contrasting species; long history of development and application; ease of parameterization	Requires numerical integration for volume estimates; can have high multicollinearity; can have unstable behavior near stem base	Newnham (1992); Kozak (1988, 2004)
Compatible	Long history of development with consistent linkages between stem form and volume; often has algebraically integration; can be estimated as a system of equations	May constrain behavior and unnecessarily reduce flexibility with limited gains in accuracy for volume predictions; no assurance of biologically reasonable representation of stem form	Demaerschalk (1972); Fang et al. (2000); Sharma and Oderwald (2001)
Polynomial	Ease of fit and application; continuous with a single equation required; algebraically integrable and invertible; consistent	Often requires numerous constraints for proper behavior; can overfit and not extrapolate well	Kozak et al. (1969); Goodwin (2009); Téo et al. (2018)
Segmented	Long history of development and still widely used today; ensures proper and biologically consistent behavior; algebraically integrable and invertible	Noncontinuous; determination and estimation of optimal join points can be challenging	Max and Burkhart (1976); Clark et al. (1991); Valentine and Gregoire (2001)
Trigonometric	Flexible and potentially more parsimonious than variable-form approaches; robust for species with complex forms; biological interpretability; algebraically integrable and invertible	May reduce flexibility; can be noncontinuous and inconsistent in behavior	Matney et al. (1985); Thomas and Parresol (1991); Bi (2000)
Matrix	Simple yet robust formulation; relies on within-tree relationships; can incorporate additional predictors	Limited application; reliance on upper-stem diameters	Kilkki et al. (1978)

log length and g_m is the cross-sectional area of the log at mid-length).

2.3. Modern taper equation forms

Since the 1960s, there has been a preference for mathematically based model forms that offer the flexibility needed to accurately estimate stem taper yet are constrained to ensure proper behavior from the ground to tree tip. The vast majority of stem taper equations rely primarily on three predictors (i.e., relative or absolute height in the stem (h_u), DBH, and H), despite a variety of additional model predictors that have been tested with differing degrees of improvement. In contrast, a wide variability of stem taper equation model forms have been developed and used, but most are of four primary types: (*i*) variable-form; (*ii*) compatible and parsimonious; (*iii*) polynomial, segmented, and splines; and (*iv*) trigonometric and matrix. These types are further described and compared in the following sections (Table 1).

2.3.1. Variable-form taper functions

Recognizing the drawback of assigning a unique shape variable, or r exponent of eq. 4, to the entire tree stem profile, numerous authors have indicated that a typical tree is a composite of several geometric forms and segments. As depicted in Fig. 4, the typical tree contains a bottom log that resembles frustums of a neiloid, several logs or bolts in the middle portion of the tree possessing the shape of a paraboloid, and the tip of the tree that is often conic in shape. Based on a sample size of 11 000 first (butt) logs, Bruce (1982) affirmed the approximate neiloid shape for the first (butt) log of multiple species in the US Pacific Northwest and derived a cubic volume equation for the first log as $v_{butt} = L \times (0.25 \times g_a + 0.75 \times g_b)$, where L is log length and g_a and g_b are the cross-sectional areas of the log for the lower and upper end, respectively. The empirical Bruce (1982) formula contains less volume than the exact Grosenbaugh (1966) formula for a frustum of a neiloid, which is expressed as $v = k \times L\left[d_a d_b + \frac{(d_a - d_b)^2}{4}\right]$, where $k = \pi/40\,000$ and d_a and d_b are the diameters of the log for the lower and upper end, respectively. It exceeds the Bruce (1982) formula for first log by the quantity $0.5 \times k \times L \times d_b(d_a - d_b)$. The observed volume of logs or bolts in the middle section of the tree is parabolic, which is typically computed with the Smalian formula or $v_{middle} = L \times (0.5 \times g_a + 0.5 \times g_b)$. The observed volume of the log at the tip of the tree is conic, which is computed as $v_{tip} = (L/3) \times g_a$. The taper function constructed by Fang et al. (2000) implicitly produced an empirical volume formula for slash pine (*Pinus elliottii* Engelm.) at the tip of a tree. The approximate Fang et al. (2000) volume formula for the top segment of the tree is expressed as $v_{tip} = (L/2.604) \times g_a$.

Inspecting Fig. 4, Newnham (1988, 1992) suggested that eq. 4 should no longer be deployed for a tree of interest using one constant value for the exponent r. Rather, the changing shape and implied value of r for each stem segment could be represented with changing step values. Newnham transformed eq. 4 and placed the exponent governing stem form on the left-hand side:

$$(7) \qquad \left(\frac{d_u}{DBH}\right)^k = \left(\frac{H - h_u}{H - 1.3}\right)$$

where $k = 2/r$ of eq. 4; $k = 1$ is a cone, $k = 2$ is a quadratic paraboloid, $k = 3$ is a cubic paraboloid, and $k = 2/3$ is a neiloid. The changing step values of k, by geometric shape for each stem segment, are represented in Fig. 5. It is easy to obtain an observed value for k at each bolt cut of a sample tree, computed as

$$(8) \qquad k = \frac{\ln\left(\frac{H - h_u}{H - 1.3}\right)}{\ln\left(\frac{d_u}{DBH}\right)}$$

Newnham (1988, 1992) then constructed regression equations for the exponent k as a function of relative height $\left(\frac{H - h_u}{H - 1.3}\right)$ and the slenderness ratio (DBH/H):

Fig. 4. The relative height of the dashed lines denotes the gradual transition in geometric shapes from cone to paraboloid to neiloid. Figure was adapted from Newnham (1988).

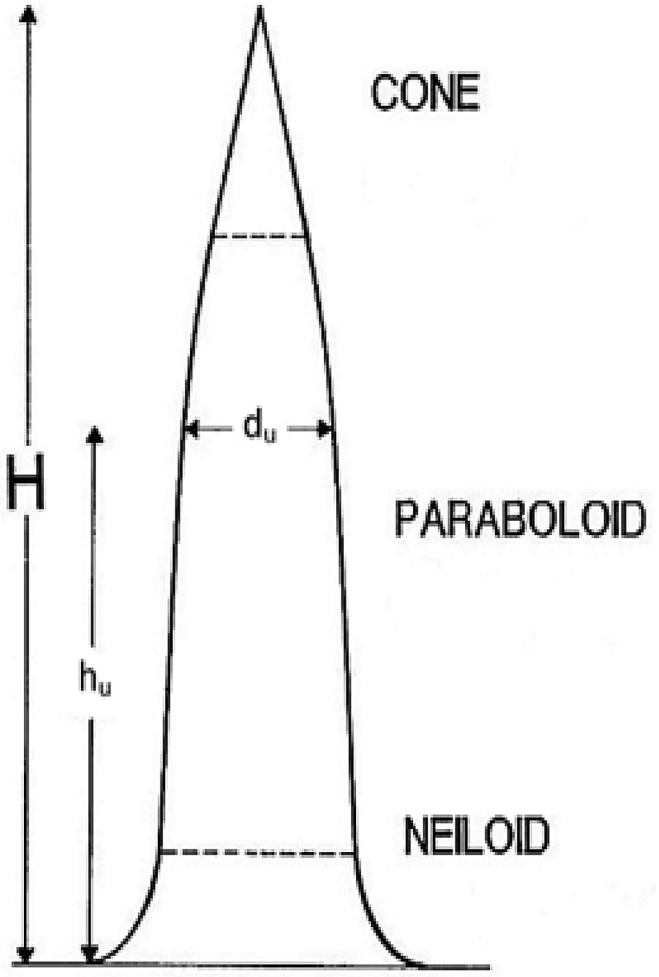

$$k = 2.48 - 1.540 \times \left(\frac{H - h_u}{H - 1.3}\right)^6 - 0.696 \times \frac{DBH}{H} + 0.770 \times \left(\frac{H - h_u}{H - 1.3}\right)^2 \frac{DBH}{H} \quad (9)$$

Figure 5 contains the hypothesized continuous shape values for k; however, it shows them only as a function of relative height. Predicted values for upper-stem diameter are then calculated as

$$\hat{d}_u = DBH \times \left(\frac{H - h_u}{H - 1.3}\right)^{1/k} \quad (10)$$

If the exponent $1/k$ in eq. 10 is a function of one constant parameter, as in the case of the simple Ormerod (1973) model, it is no longer considered as a variable-form taper function. Similar to the Ormerod (1973) taper model, the Behre (1927) hyperboloid is another simple one-parameter model that can be expanded as a variable-form taper function. With some modifications of the Bruce (1972) terminology, the Behre (1927) taper model is expressed as

$$\frac{d_u}{DBH} = \frac{H - h_u}{H - \alpha h_u} \quad (11)$$

Fig. 5. Relationship between $k = 2/r$ of eq. 4 and the domain for relative height extended beyond the 0–1 range of original taper function of eq. 4. The continuous curve implies a gradual transition for change in taper and form for the stem bole with changes in relative height. Figure from Newnham (1988).

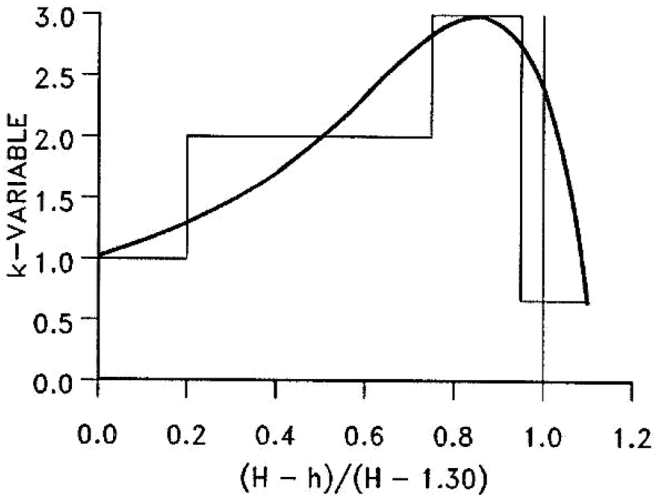

where $0 \le \alpha \le 1$. When $\alpha = 0$, the stem resembles a cone, whereas the stem resembles a cylinder when $\alpha = 1$. Bruce (1972) demonstrated that the parameter α could be observed for each bolt cut of a sample tree with the computation

$$\alpha = \frac{Hd_u - DBH(H - h_u)}{d_u h_u} \quad (12)$$

Similar to eq. 9, a prediction equation can then be constructed for the Behre (1927) parameter α, making it a variable-form taper function.

Variable-form taper functions were considerably advanced by Kozak (1988) using one continuous function to describe the shape of the bole with a changing exponent to compensate for the neiloid, paraboloid, and conic forms. Kozak (1988) started with the premise that the upper-stem diameter profile was guided by the inflection point where the stem changes from a neiloid to a paraboloid:

$$\frac{d_u}{DBH} = X^c \quad (13)$$

where $X = \frac{1 - (h_u/H)^\eta}{1 - p^\eta}$; $\eta = 0.5$; p is the relative height (h_u/H) of the inflection point, typically 20%–25% of total height; and C is a continuous function for the entire stem, consisting of polynomials and transformations of relative height and the slenderness ratio. The change in direction from a neiloid to paraboloid occurs at the relative height p when $X = 1.0$. Kozak (2004) provides a good summary of successive changes to eq. 13 over time; however, the basic behavior of the model remains unchanged because it is governed by the X variable. Several enhancements have also been implemented with respect to the C exponent function. The latest model identified by Kozak (2004) has the following formulation:

$$d_u = a_0 DBH^{a_1} H^{a_2} X^{\left(b_1 z^4 + \frac{b_2}{e^{DBH/H}} + b_3 X^{0.1} + \frac{b_4}{DBH} + b_5 H^Q + b_6 X\right)} \quad (14)$$

where $z = h_u/H$, $\eta = 1/3$, $p = 1.3/H$, $Q = 1 - (h_u/H)^\eta$, and a_i and b_i are coefficients determined from regression. Indeed, in more recent

Fig. 6. The Kozak (2004) formulation (eq. 14) is well suited for testing hypotheses in the *C* exponent function. Li et al. (2012) used an indicated variable for stand origin and determined large differences in the stem profile by relative height for natural and planted red spruce (*Picea rubens* Sarg.). Figure was adapted from Li et al. (2012).

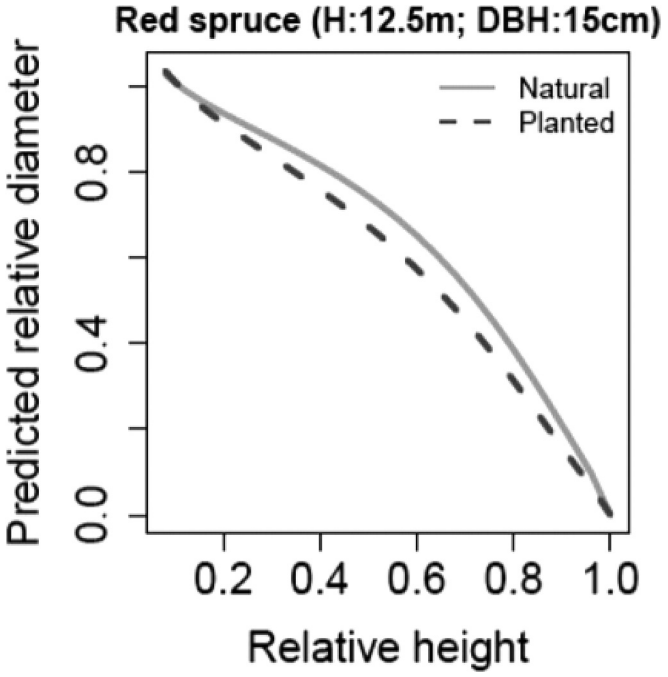

applications of the Kozak (2004) taper function outside of North America's Pacific Northwest, it is now common to encounter the value of the inflection point set to $p = 1.3/H$ and the power of the inflection point set to $\eta = 1/3$ (Li et al. 2012; Weiskittel and Li 2012; Scolforo et al. 2018), and the term for tree size, namely $a_0\text{DBH}^{a_1}H^{a_2}$, has also improved performance (Kozak 2004). The exponent terms inside the parentheses of eq. 14 correspond to the *C* exponent function of eq. 13, which is ideally suited for testing additional hypotheses regarding stem form. For instance, Li et al. (2012) found that stand origin (planted vs. natural) had a rather large effect on the stem profile across several softwood species in eastern North America (Fig. 6).

Equation 14 possesses less multicollinearity than earlier models. Although the model initially appears complex, it can be easily transformed to a linear model by applying logarithms. The initial parameter values obtained from linear regression considerably facilitate the nonlinear regression fitting of eq. 14. It should be noted that eq. 14 must be inverted by an iterative numerical procedure to compute h_u as a function of d_u. Likewise, numerical integration must be employed to compute stem volume. Neither numerical task is very difficult, and Robinson and Hamann (2011) demonstrated the uniroot function in R software for inverting the taper function with the Kozak (2004) model. In addition, most studies comparing multiple taper model forms have found variable-form to perform the best in predicting both stem profile and volume (Rojo et al. 2005; Li and Weiskittel 2010).

2.3.2. *Compatible and parsimonious taper functions*

Compatibility implies that the integration of the taper function over the domain of ground line to total height will produce an estimate that equals that of a total volume equation. Compatibility can be a useful and expedient feature, especially if it can produce a taper function that requires no fitting. Ultimately, however, a fitted taper model with d_u as the dependent variable will outperform a compatible profile equation with parameters that are indirectly derived from a total or merchantable volume equation. As highlighted by Zhao et al. (2019), compatibility can be defined both in algebraic terms as well as numerical consistency among the components of total volume, merchantable volume, and taper.

Demaerschalk (1972) introduced a clever technique to produce a taper function that is compatible with the popular Spurr (1952) total volume equation, namely, $v = a_0 + a_1 \times \text{DBH}^2 \times H$. The Demaerschalk (1972) taper function is expressed as

$$(15)\qquad \left(\frac{d_u}{\text{DBH}}\right)^2 = \frac{a_0(b_1+1)}{k\text{DBH}^2H}\times\left(\frac{H-h_u}{H}\right)^{b_1} + \frac{a_1(b_2+1)}{k}\times\left(\frac{H-h_u}{H}\right)^{b_2}$$

where $k = \pi/40\ 000$, a_i are predetermined or exogenous coefficients of the Spurr (1952) volume equation, and b_i are "free" coefficients estimated from nonlinear regression. Recognizing that total volume is computed as $v = k\int_0^H d_u^2 dh_u$, it follows that compatibility is attained with the integration of eq. 15, resulting in

$$(16)\qquad v = \frac{a_0(b_1+1)}{H^{b_1+1}}\left[-\frac{(H-h_u)^{b_1+1}}{b_1+1}\right]_0^H + \frac{a_1(b_2+1)\text{DBH}^2}{H^{b_2}}\times\left[-\frac{(H-h_u)^{b_2+1}}{b_2+1}\right]_0^H$$

After simplification, eq. 16 results in $v = a_0 + a_1 \times \text{DBH}^2 \times H$. Goulding and Murray (1976) used a fifth-degree linear polynomial taper function to achieve compatibility. The left-hand side is a unitless value, as it represents the subtraction of the relative height from relative volume (tip to base). Total volume (v) is a predetermined or exogenous value:

$$(17)\qquad \frac{d_u^2kH}{v} - 2z = b_1(3z^2-2z) + b_2(4z^3-2z) + b_3(5z^4-2z) + b_4(6z^5-2z)$$

where $z = (H - h_u)/H$. Moving $2z$ to the right-hand side and multiplying both sides by v, it follows that compatible volume is demonstrated using a change of variable technique, so that $dz = -dh_u/H$. The limits of integration are no longer h_u from 0 to H, but rather z from 1 to 0.

$$(18)\qquad v = -kH\int_{h_u=0}^{h_u=H} d_u^2\left(-\frac{dh_u}{H}\right) = -kH\int_1^0 d_u^2 dz$$

therefore,

$$(19)\qquad v = -b_1v[z^3-z^2]_1^0 - b_2v[z^4-z^2]_1^0 - b_3v[z^5-z^2]_1^0 - b_4v[z^6-z^2]_1^0 - 2v\left[\frac{z^2}{2}\right]_1^0$$

Equation 19 results in $v = v$. Reed and Green (1984) created a compatible taper function that is identical to the Demaerschalk (1972) profile function (eq. 15) with two exceptions: (*i*) the a_0 coefficient of the Spurr (1952) combined variable volume equation was set to zero and (*ii*) the a_1 coefficient of the Spurr (1952) model was estimated simultaneously in a system of equations. The Sharma and Oderwald (2001) compatible taper model shares

Fig. 7. Comparison of tree taper function for a Chinese fir with a diameter at breast height (DBH) of 20 cm, total height (H) of 21 m, and quadratic mean diameter (Dg) of 17.5 cm. The compatible taper function with zero "free" coefficients (eq. 22) predicts a d_u of 5 cm at a height of 20 m, whereas the modified Brink and von Gadow (1983) model predicts a d_u of 2 cm at a height of 20 m. Note that primary differences are at the stem base and near the tree tip. Equation 22 does not possess a mathematical formulation that is capable of flaring at the base of the tree. [Color online.]

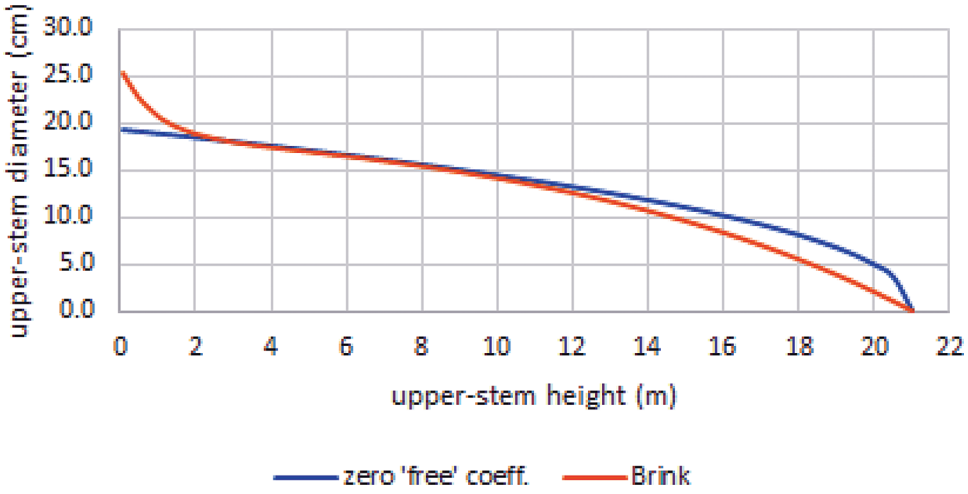

several features of the Reed and Green (1984) system, especially with respect to parsimony. Sharma and Oderwald (2001) presented the following one-parameter taper equation that is constrained to predict that d_u = DBH when h_u = 1.3:

$$d_u^2 = \mathrm{DBH}^2 \left(\frac{h_u}{1.3}\right)^{2-\gamma} \left(\frac{H-h_u}{H-1.3}\right) \quad (20)$$

Equation 20 is compatible with the volume equation, $v = \beta \times \mathrm{DBH}^{\gamma} \times H^{3-\gamma}$, provided that volume and upper-stem diameter are simultaneously estimated in a system with the following constraint: $\beta = \dfrac{k \times \left[\left(\dfrac{\mathrm{DBH}}{1.3}\right)^{2-\gamma} \Big/ \left(1-\dfrac{1.3}{H}\right)\right]}{(3-\gamma)\times(4-\gamma)}$, where $k = \pi/40\,000$. The equations of Demaerschalk (1972), Reed and Green (1984), and Sharma and Oderwald (2001) are all quite similar, especially if $\gamma \approx 2$ in eq. 20. Parsimony and compatibility appear to be the main advantage in these models, but the parsimonious and compatible model loses its accuracy if taken too far. For example, von Gadow and Hui (1999) presented the following Schumacher and Hall (1933)–type total volume inside bark equation for Chinese fir (*Cunninghamia lanceolata* (Lamb.) Hook.) in China:

$$v = b_0 \times \mathrm{DBH}^{b_1} \times H^{b_2} \quad (21)$$

where b_0 = 0.000058777, b_1 = 1.9699831, and b_2 = 0.89646157.

Employing the Demaerschalk (1972) technique, a compatible taper function for eq. 21 with essentially zero "free" parameters would be

$$d_u = \sqrt{\frac{b_0 \times (b_2+1) \times \mathrm{DBH}^{b_1} \times (H-h_u)^{b_2}}{k \times H}} = 1.19133 \times \mathrm{DBH}^{0.9850} \times (H-h_u)^{0.4482} \times H^{-0.5} \quad (22)$$

Equation 22 is a compatible taper function; however, its usefulness is potentially limited, as the mathematics of consistent integration are no guarantee of biological realism in a stem profile. Von Gadow and Hui (1999) conducted a comparison between the estimates of total volume obtained from eq. 21 and a closed-form integral of the modified Brink and von Gadow (1983) taper model as presented by Riemer et al. (1995). Despite the outstanding properties of the Brink and von Gadow model, it is not a compatible taper equation. The modified Brink and von Gadow taper model is expressed as

$$d_u = 2\left(u + v e^{-p h_u} - w e^{q h_u}\right) \quad (23)$$

where $u = \dfrac{i}{1-e^{q\times(1.3-H)}} + \left(\dfrac{\mathrm{DBH}}{2} - i\right)\left[1 - \dfrac{1}{1-e^{p\times(1.3-H)}}\right]$, $v = \dfrac{[(\mathrm{DBH}/2)-i]\times e^{p\times 1.3}}{1-e^{p\times(1.3-H)}}$, $w = \dfrac{i \times e^{-qH}}{1-e^{q\times(1.3-H)}}$, $i = 0.40788 \times \mathrm{DBH}^{1.03702}$, $p = e^{(1.79624/\mathrm{Dg})}$, $q = 10.43850 \times e^{(-1.41743/\mathrm{Dg})} \times H^{-1.50117}$, and Dg is quadratic mean diameter in centimetres, which is an auxiliary variable that is available from most forest inventories. Figure 7 presents a comparison between the modified Brink and von Gadow (1983) taper function (eq. 23) and the compatible taper function with zero "free" coefficients (eq. 22). As noted by von Gadow and Hui (1999), a major application of taper functions is the merchandizing of multiple stem products, so the ability to accurately predict upper-stem diameter over the entire stem profile is of paramount importance.

Another important category of compatible taper models is derived from merchantable volume ratio models. The ratio models are extremely useful given changing markets and the common occurrence of new merchantability specifications for products. The ratio models avoid illogical crossover in volume estimates that occur when several independently fit equations are used to estimate volumes to multiple top diameters. Two common ratio models are the Burkhart (1977) and the Cao and Burkhart (1980) formulations (eqs. 24 and 25, respectively):

$$\frac{v_m}{v} = 1 - a_0 \frac{d_u^{a_1}}{\mathrm{DBH}^{a_2}} \quad (24)$$

$$\frac{v_m}{v} = 1 - b_0 \frac{(H-h_u)^{b_1}}{H^{b_2}} \quad (25)$$

where v_m is cumulative merchantable volume from the ground line or stump to either d_u or h_u. Experience has demonstrated that eq. 25 is more precise than eq. 24 (Tasissa et al. 1997; Bullock and Burkhart 2003); however, both equations are typically needed for merchandizing multiple products when specifications are in terms of product length and diameter at the small end of the log. At the tip of the tree, v_m is conditioned to equal v in both eqs. 24 and 25. Burkhart and Tomé (2012) demonstrated that by equating the right-hand side of eqs. 24 and 25, it is possible to derive a taper function:

$$d_u = \left[\frac{b_0 \times (H - h_u)^{b_1} \mathrm{DBH}^{a_2}}{a_0 \times H^{b_2}}\right]^{1/a_1} \quad (26)$$

Equation 26 is a noncompatible taper function, as it was derived from algebraic rearrangement of two ratio models. However, Bullock and Burkhart (2003) have demonstrated that it performs reasonably well in predicting d_u, and eq. 26 can be easily inverted to predict h_u as a function of d_u. Similarly, Clutter (1980) noted that merchantable volume (v_m) of eq. 24 also equals a solid of revolution descending from the tree tip:

$$v_m = v - v \times a_0 \times \frac{d_u^{a_1}}{\mathrm{DBH}^{a_2}} = v - k\int_0^T d_o^2 \mathrm{d}t \quad (27)$$

where T is distance from the tip of tree to d_u ($h_u + T = H$), and $d_o^2 = f(t)$ shows that diameter squared descending the stem is a function of t, ($0 \le t \le T$). When $t = T$, then $d_u = [f(T)]^{0.5}$. When eq. 27 is rearranged as

$$k\int_0^T f(t)\mathrm{d}t = va_0 \frac{[f(T)]^{0.5a_1}}{\mathrm{DBH}^{a_2}} \quad (28)$$

differentiating both sides of eq. 28, and using the fundamental theorem of calculus, results in

$$kf(T) = va_0(0.5a_1)\frac{[f(T)]^{0.5a_1-1}}{\mathrm{DBH}^{a_2}}\frac{\mathrm{d}[f(T)]}{\mathrm{d}T} \quad (29)$$

Separation of the term dT to the left-hand side of the equation and the terms involving $f(T)$ to the right-hand side of the equation provides

$$\frac{2k\mathrm{DBH}^{a_2}}{va_0a_1}\mathrm{d}T = [f(T)]^{0.5a_1-2}\mathrm{d}[f(T)] \quad (30)$$

A separable differentiation technique may be used to solve explicitly for $f(T)$ or d_u^2.

$$\frac{2k\mathrm{DBH}^{a_2}}{va_0a_1} \times T = \frac{\left[f(T)^{0.5a_1-1}\right]}{0.5a_1 - 1} + c \quad (31)$$

where c is a constant of integration.

Imposing conditions on the constant of integration that $T = 0$ when $f(T) = 0$, and recognizing that $T = H - h_u$, provides the following after rearrangement:

$$d_u = \left[\frac{k \times (H - h_u) \times \mathrm{DBH}^{a_2} \times (a_1 - 2)}{v \times a_0 \times a_1}\right]^{1/(a_1-2)} \quad (32)$$

Equation 32 can be easily inverted to predict h_u as a function of d_u. McTague and Bailey (1987) expanded upon the Clutter (1980) methodology and created a taper function with an inflection point for loblolly pine (*Pinus taeda* L.) in Brazil that was constrained to predict that d_u = DBH when h_u = 1.3 m. As Burkhart and Tomé (2012) highlighted, the merchantable volume ratio equation based on upper-stem diameter (eq. 24) can lead to some negative estimates of merchantable volume (v_m) in the lower portion of the stem. This problem is rectified by using an exponential ratio equation that is constrained to predict positive values of v_m.

$$\frac{v_m}{v} = \mathrm{e}^{\beta_1 d_u^{\beta_2} \mathrm{DBH}^{\beta_3}} \quad (33)$$

where $\beta_3 < 0$. Jordan et al. (2005) derived a parsimonious and compatible taper function using the merchantable volume ratio model of eq. 33. Employing the approach of Clutter (1980), they determined that volume at the tip of the tree downward was equivalent to

$$k\int_0^T f(t)\mathrm{d}t = v - v \times \mathrm{e}^{\beta_1 d_u^{\beta_2} \mathrm{DBH}^{\beta_3}} \quad (34)$$

Using the transformation, $x = d_u^{\beta_2}$, they determined that

$$kT = -v\frac{\beta_1 \mathrm{DBH}^{\beta_3}\beta_2}{2}\int_0^{d_u^{\beta_2}} x^{1-(4/\beta_2)} e^{\beta_1 x \mathrm{DBH}^{\beta_3}} \frac{2}{\beta_2} x^{(2/\beta_2)-1}\mathrm{d}x \quad (35)$$

With the additional transformation of $z = -\beta_1 x \times \mathrm{DBH}^{\beta_3}$, $dz = -\beta_1 \mathrm{DBH}^{\beta_3}\mathrm{d}x$, it follows that

$$kT = v\left(-\beta_1 \mathrm{DBH}^{\beta_3}\right)^{2/\beta_2}\int_0^{-\beta_1 d_u^{\beta_2}\mathrm{DBH}^{\beta_3}} z^{[(\beta_2-2)/\beta_2]-1}\mathrm{e}^{-z}\mathrm{d}z \quad (36)$$

This leads to

$$k(H - h_u) = v\left(-\beta_1 \mathrm{DBH}^{\beta_3}\right)^{2/\beta_2}\gamma\left(\frac{\beta_2 - 2}{\beta_2}, -\beta_1 d_u^{\beta_2}\mathrm{DBH}^{\beta_3}\right) \quad (37)$$

where γ is a lower incomplete gamma function with $\gamma(\alpha, x) = \Gamma(\alpha)\mathrm{F}(x)$, and $\mathrm{F}(x)$ is the cumulative distribution function (cdf) of the gamma. The compatible taper function is finally expressed as

$$d_u = \Gamma^{-1}\left[\frac{\beta_2 - 2}{\beta_2}, \frac{k(H - h_u)}{v\left(-\beta_1 \mathrm{DBH}^{\beta_3}\right)^{2/\beta_2}\Gamma\left(\frac{\beta_2-2}{\beta_2}\right)}\right]^{1/\beta_2} \times \left(\frac{1}{-\beta_1 \mathrm{DBH}^{\beta_3}}\right)^{1/\beta_2} \quad (38)$$

Seemingly unrelated regression (SUR) can be employed to conduct a simultaneous fit of the merchantable volume ratio equation (eq. 33) and the taper function (eq. 38) for the three β_i coefficients. The system is parsimonious and compatible, possesses acceptable fit statistics, and does not require numerical integration techniques for estimating volume. In contrast, the authors of this paper have employed another parsimonious taper function that is considerably easier to fit than that of the Jordan et al. (2005) model and is superior in performance. Using the approach and statistical source code provided by Harrell (2015), the authors fit eq. 39 with a restricted cubic spline (RCS) to 183 clonal trees of the genus *Eucalyptus* L'Hér. from Água Clara, Mato Grosso do Sul, Brazil. The data used to fit eq. 39 are described by Scolforo et al. (2018). Equations 33 and 38 were simultaneously fit to the same data, and the two taper functions are compared in Fig. 8. The fitted RCS model contains four knots but, after several restrictions, possesses only three coefficients. In addition to setting the intercept to zero, the constraints ensure better behavior in the tails, that is, before the first knot and after the last knot (Harrell 2015).

Fig. 8. Stem profile equations for clonal eucalyptus with a DBH of 20 cm and H of 26 m. Both models possess three fitted coefficients; however, the restricted cubic spline (RCS) model is considerably more precise in predicting upper-stem diameter than the Jordan et al. (2005) model. [Color online.]

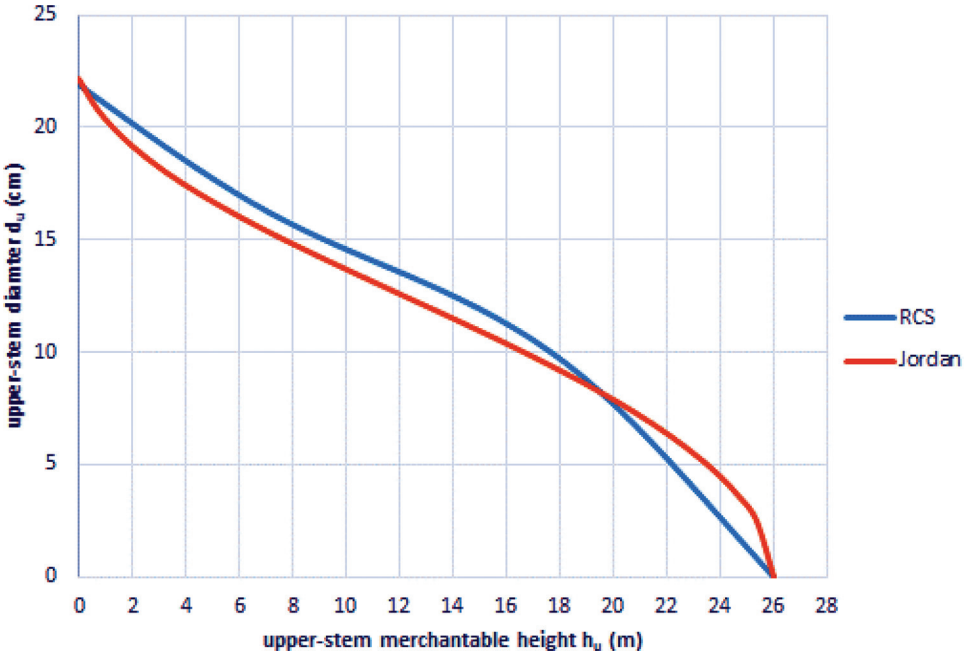

$$\frac{d_u}{DBH} = \beta_1\left(\frac{H-h_u}{H}\right) + \beta_2\left(\frac{H-h_u}{H} - 0.077\right)_+^3 + \beta_3\left(\frac{H-h_u}{H} - 0.272\right)_+^3 + \beta_4\left(\frac{H-h_u}{H} - 0.717\right)_+^3 + \beta_5\left(\frac{H-h_u}{H} - 0.975\right)_+^3 \quad (39)$$

where the knot values of 0.077, 0.272, 0.717, and 0.975 correspond to the 5th, 25th, 60th, and 90th percentiles of $(H - h_u)/H$, respectively. The subscript operator "+" implies that the function is only computed when the value of $(H - h_u)/H$ is larger than the knot value inside the parentheses. In reality, only the β_1, β_2, and β_3 coefficients are estimated. Harrell (2015) presented a new term τ, which is the square of the last knot value minus the first knot value; $\tau = (0.975 - 0.077)^2$. β_1 remains unchanged, but β_2 and β_3 now become $\beta_2^* = \frac{\beta_2}{\tau}$ and $\beta_3^* = \frac{\beta_3}{\tau}$, respectively. β_4 and β_5 are computed as $\beta_4 = \frac{\beta_2^*(0.077 - 0.975) + \beta_3^*(0.272 - 0.975)}{0.975 - 0.717}$ and $\beta_5 = \frac{\beta_2^*(0.077 - 0.717) + \beta_3^*(0.272 - 0.717)}{0.717 - 0.975}$, respectively. Upper-stem diameter d_u is now predicted using eq. 39 and the previously determined values of β_1, β_2^*, β_3^*, β_4, and β_5. The 183 sample trees of clonal eucalyptus were cut into 2 m bolts, resulting in 2851 observations. Inspecting the sum of squares of error (SSE) for upper-stem diameter, or $\Sigma(d_u - \hat{d}_u)^2$, the RCS eq. 39 resulted in a reduction of 22% in SSE when compared with eq. 38.

In contrast to the Clutter (1980) approach, which is based on relative diameter, both Van Deusen et al. (1982) and Lynch et al. (2017) found it considerably easier to derive compatible taper functions from merchantable volume ratio models that are based on relative height. Rather than approaching the solid of revolution from the tip of the tree downward, Van Deusen et al. (1982) defined merchantable volume from the base of the stem upward:

$$v_m = k\int_0^{h_u} d_u^2 dh_u \quad (40)$$

Dividing both sides by k and applying a derivative to both sides results in

$$d_u^2 = \frac{d}{dh_u}\left[\frac{v_m(h_u)}{k}\right] \quad (41)$$

Van Deusen et al. (1982) elected to work with a simple volume ratio model as a function of relative height. Their ratio model is constrained so that when merchantable height h_u equals the stump height of 15 cm, the merchantable volume (v_m) equals zero.

$$v_m(h_u) = v - v \times \left[\frac{H - h_u}{H - 0.15}\right]^c \quad (42)$$

where c is an estimated coefficient. Applying eq. 41 results in the following compatible taper function:

$$d_u^2 = \frac{v \times c(H - h_u)^{c-1}}{k(H - 0.15)^c} \quad (43)$$

Lynch et al. (2017) employed the same technique as that of Van Deusen et al. (1982) and derived a compatible taper function from the original merchantable volume ratio equation developed by Cao and Burkhart (1980) (eq. 25). Lynch et al. demonstrated a compatible taper function for eq. 25 that is expressed as

$$d_u = \sqrt{-\frac{v \times b_0 \times b_1}{k}\frac{(H - h_u)^{b_1 - 1}}{H^{b_2}}} \quad (44)$$

This equation can be easily inverted to predict h_u as a function of d_u:

$$(45)\qquad h_u = H - \left[\frac{-k \times d_u^2 \times H^{b_2}}{v \times b_0 \times b_1}\right]^{1/(b_1-1)}$$

Additionally, Lynch et al. (2017) derived a new merchantable volume ratio model, $v_m(h_u)$, based on relative height that produced a better taper function. Using the principles previously outlined, Lynch et al. (2017) recommended the following merchantable volume ratio model:

$$(46)\qquad v_m(h_u) = a_0 \times \mathrm{DBH}^{a_1} \times H^{a_2} - c_0 \times \mathrm{DBH}^{c_1} \times H^{c_2}\left(1 - \frac{h_u}{H}\right)^{\alpha}$$

The first term of the right-hand side of eq. 46, $a_0\mathrm{DBH}^{a_1}H^{a_2}$, is the expression for total volume, v. A compatible taper function for eq. 46 is easily derived as

$$(47)\qquad d_u = \sqrt{\frac{\alpha}{kH} c_0 \mathrm{DBH}^{c_1} H^{c_2}\left(1 - \frac{h_u}{H}\right)^{\alpha-1}}$$

Compatible model forms offer the advantage of ensuring optimized estimates of both stem form and volume, which are often not potentially ensured by other methods. Recently, Zhao et al. (2019) demonstrated the ability to have a completely compatible system of taper, total, and merchantable volume equations that are algebraically compatible and numerically consistent among all component equations. In this analysis, simultaneous parameter optimization of both taper and cumulative volume was preferable to separate optimization for taper or volume only (Zhao et al. 2019). The approach of Zhao et al. (2019) was extended to several *Pinus* L. species in Mexico and found to outperform the other compatible taper and volume systems (Quionez-Barraza et al. 2019). Although they may not provide the best predictions of either form or volume (Li and Weiskittel 2010), some analyses indicate that they can be one of the best performing approaches (e.g., Shahzad et al. 2020).

2.3.3. Polynomials, segmented models, and splined taper functions

Over several decades in North America, many individuals were first introduced to taper functions with the Kozak et al. (1969) second-degree polynomial equation as an example:

$$(48)\qquad \left(\frac{d_u}{\mathrm{DBH}}\right)^2 = a_0 + a_1 \times \frac{h_u}{H} + a_2 \times \left(\frac{h_u}{H}\right)^2$$

Equation 48 is linear with respect to the parameters, is invertible for computing h_u as a function of d_u, and can be integrated with an analytical solution for computing volume. Avery and Burkhart (2002) demonstrated that when eq. 48 is integrated to compute total volume, the expression is a Spurr (1952)–type of combined variable equation because it does not contain an intercept ($v = a_1 \times \mathrm{DBH}^2 \times H$). Although third-degree and higher order polynomials will lead to a better fit, it can prompt some oscillation in the fitted function when the domain of the independent variable has a range of [0, 1]. In Brazil, the fifth-degree polynomial remains a popular model for taper, primarily for its ease of parameter estimation with linear regression (Téo et al. 2018). Typically, however, it is fit without the square power for the dependent variable (Téo et al. 2018):

$$(49)\qquad \frac{d_u}{\mathrm{DBH}} = \beta_0 + \beta_1 \times \left(\frac{h_u}{H}\right) + \beta_2 \times \left(\frac{h_u}{H}\right)^2 + \beta_3 \times \left(\frac{h_u}{H}\right)^3 + \beta_4 \times \left(\frac{h_u}{H}\right)^4 + \beta_5 \times \left(\frac{h_u}{H}\right)^5$$

Scolforo et al. (2018) fit eq. 49 to the clonal eucalyptus data set highlighted in the previous section and obtained the following predicted taper function:

$$(50)\qquad \frac{d_u}{\mathrm{DBH}} = 1.149 - 3.4350 \times \left(\frac{h_u}{H}\right) + 16.0934 \times \left(\frac{h_u}{H}\right)^2 - 38.7426 \times \left(\frac{h_u}{H}\right)^3 + 40.4870 \times \left(\frac{h_u}{H}\right)^4 - 15.5778 \times \left(\frac{h_u}{H}\right)^5$$

Figure 9 displays the predicted value of eq. 50 for a sample tree with a DBH of 20 cm and total height (H) of 26 m. An illogical shape is evident for the stem section between 6 and 16 m in height (Fig. 9), and the function also has the drawback of predicting a negative d_u value at the tip of the tree. This drawback is easily avoidable by imposing a restriction on the β_0 parameter such that $d_u = 0$ when $h_u = H$. This constraint redefines the independent variables as $\left(\frac{H - h_u}{H}\right)^p$, where p is the degree of the polynomial power. As displayed in Fig. 9, the oscillating residual pattern of eq. 50 persists as a concern. The fifth-degree polynomial can be improved substantially when estimating upper-stem diameter if some of the integer power terms of eq. 49 are replaced with real numbers below 1.0 (Hradetzky 1976). When fit to the same clonal eucalyptus data set of Scolforo et al. (2018), the following taper model reduced the SSE by 22% when compared with eq. 49:

$$(51)\qquad \frac{d_u}{\mathrm{DBH}} = \beta_0 + \beta_1 \times \left(\frac{h_u}{H}\right)^{0.00001} + \beta_2 \times \left(\frac{h_u}{H}\right)^{0.2} + \beta_3 \times \left(\frac{h_u}{H}\right)^{0.9} + \beta_4 \times \left(\frac{h_u}{H}\right)^{1} + \beta_5 \times \left(\frac{h_u}{H}\right)^{10}$$

where SSE for upper-stem diameter was defined as $\Sigma\left(d_u - \hat{d}_u\right)^2$. Equation 51 was fit with the following constraint: $\beta_0 + \beta_1 + \beta_2 + \beta_3 + \beta_4 + \beta_5 = 0$, so that the predicted taper displays logical properties at the tip of the tree. Similarly, Goodwin (2009) used a cubic polynomial model form with multiple constraints on the parameters, which was found to increase flexibility, improve predictions, and generally outperform other commonly used stem taper model forms.

Another natural approach for modeling taper has been focused on modeling each section of the stem with polynomials, or other models, and then joining them at the transition lines to account for differences in shape along the tree bole (e.g., Fig. 4). The recent nomenclature for the point of transition or join points where segments come together is to designate them as knots. The location of the transition points or knots can be either predetermined or estimated. Splined taper functions convey the image of a smooth or gradual transition from one taper segment to the next. This is enforced by conditioning each segment to have identical slope values (first or higher order derivatives) at the position of the knot.

Clark et al. (1991) constructed segmented taper functions for the major species of the southern US, which remain widely used by public agencies and the forest products industry. As displayed in Fig. 10, the tree stem is divided into four segments using three knots. The Clark et al. (1991) equations require that the user provide an estimate of inside- or outside-bark form class diameter F (d_u at 5.3 m); however, form class diameter can be predicted if it is not observed. Two of the knots — breast height (1.37 m) and form class height (5.3 m) — are predetermined, whereas the third knot is located somewhere between 40% and 70% of total stem height and is estimated from regression. Only at the third knot is the transition smooth between the two segments. The Clark et al. (1991) taper function possesses six coefficients that are species

Fig. 9. Stem profile of a fifth-degree polynomial for stem taper in eucalyptus (top). The taper model predicts that d_u = –0.5 cm when h_u = H = 26 m. The oscillating behavior for the residuals is evident in the relative height domain of $0 \le h_u/H \le 1$ (bottom).

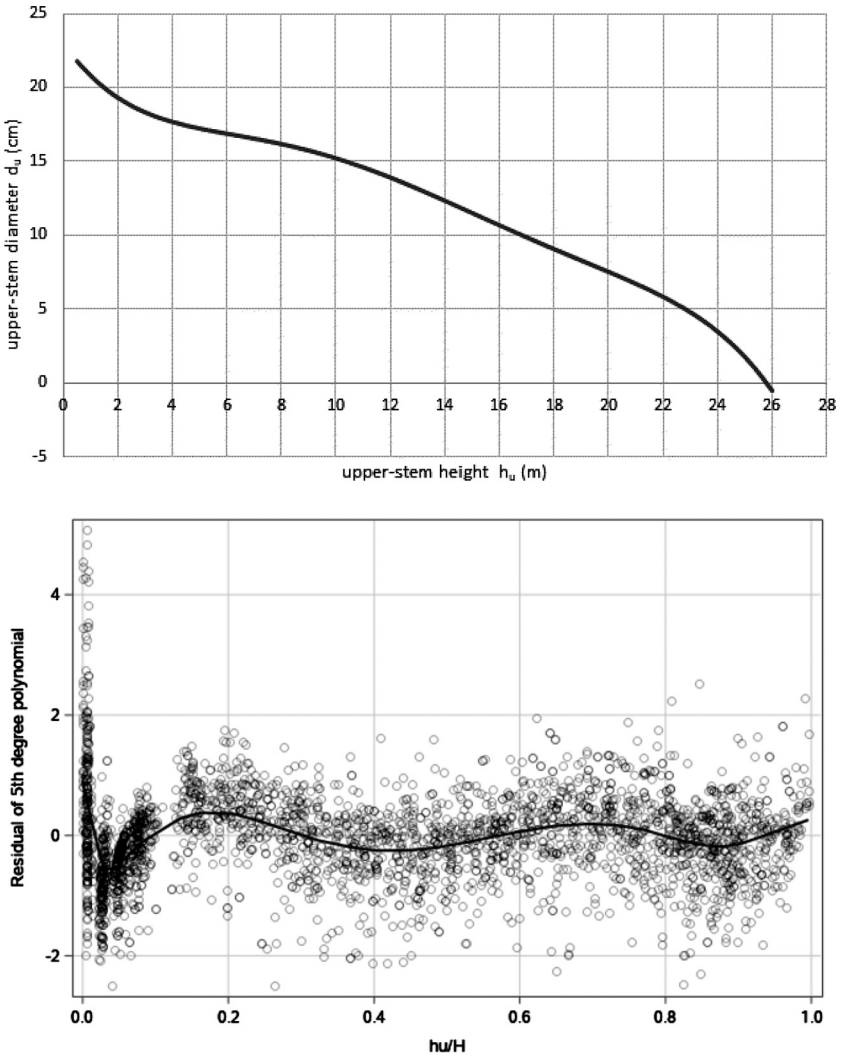

specific; however, another two species-specific coefficients are required to estimate form class diameter F if the Girard form class is unobserved (Mesavage and Girard 1946). Clark et al. (1991) declared F as the diameter (inside or outside bark) at 5.3 m above ground, and it differs slightly from the original Girard form class definition (diameter inside bark at 5.3 m divided by DBH multiplied by 100). At the base of the tree, upper-stem diameter is estimated with

$$(52) \qquad \left(\frac{d_u}{DBH}\right)^2 = 1 + \left(c + \frac{e}{DBH^3}\right)\left[\frac{\left(\frac{H-h_u}{H}\right)^r - \left(\frac{H-1.37}{H}\right)^r}{1-\left(\frac{H-1.37}{H}\right)^r}\right]$$

where r, c, and e are regression coefficients and $0\ \text{m} \le h_u \le 1.37$ m. Equation 52 is particularly well suited for species that display a buttress swell such as bald-cypress (*Taxodium distichum* (L.) Rich.) and water tupelo (*Nyssa aquatica* L.) or southern pines with less pronounced flaring at the base (Penfound 1934; Walsh and Dawson 2014). Between breast height (1.37 m) and form class height (5.3 m), upper-stem diameter is estimated with a simple interpolation function:

$$(53) \qquad \left(\frac{d_u}{DBH}\right)^2 = 1 - \left\{\frac{(DBH^2 - F^2) \times \left[\left(\frac{H-1.37}{H}\right)^p - \left(\frac{H-h_u}{H}\right)^p\right]}{DBH^2 \times \left[\left(\frac{H-1.37}{H}\right)^p - \left(\frac{H-5.3}{H}\right)^p\right]}\right\}$$

where p is a regression coefficient, F is d_u (inside or outside bark) at 5.3 m, and $1.37\ \text{m} \le h_u \le 5.3$ m. If the estimated d_u in eqs. 52 and 53 is an inside-bark value, then DBH is represented by breast-height diameter inside bark. Upper-stem diameter at 5.3 m (F) can be estimated with the following simple linear regression:

$$(54) \qquad \frac{d_{u=5.3\,m}}{DBH} = \frac{F}{DBH} = \beta_0 + \beta_1 \times \left(\frac{5.3}{H}\right)^2$$

Clark et al. (1991) indicated that they used a Max and Burkhart (1976)–type taper function for the mid-stem and upper-stem portion of the tree. Further detail about the Max and Burkhart taper model is provided later in this section; however, its base foundation in this case involves two independent second-degree polynomials of h_u/H: one for the top segment of the tree and the other for the middle segment. Clark et al. (1991) imposed four con-

Fig. 10. The Clark et al. (1991) taper function consists of four segments and three knots. Only the knot located between mid-stem and the upper stem has a smooth transition. Figure from Clark et al. (1991).

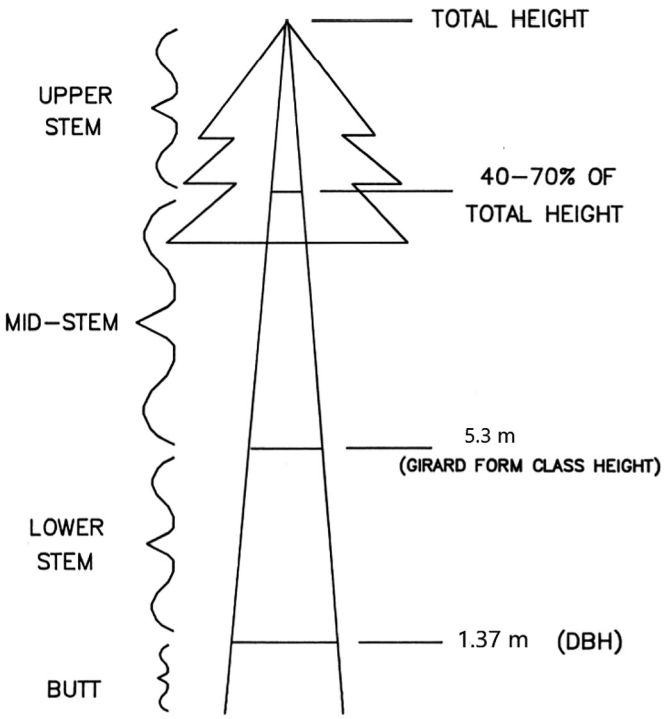

straints on the two independent polynomials and reduced a six-parameter model to a two-parameter model. The constraints involve prediction at the tip of the tree ($d_u = 0$ when $h_u = H$), prediction at form class height ($d_u = F$ when $h_u = 5.3$ m), and equivalent prediction of d_u at the knot between two segments, in addition to equal values of the first derivative at the knot. The profile model for the middle and top segments of the stem (above 5.3 m) is

$$(55)\qquad \left(\frac{d_u}{F}\right)^2 = I_m \times \left(\frac{1-b}{a^2}\right) \times \left(a - \frac{h_u - 5.3}{H - 5.3}\right)^2 + b \times \left(\frac{h_u - 5.3}{H - 5.3} - 1\right)^2$$

where a and b are regression parameters, and $I_m = 1$ if $h_u < [5.3 + a(H - 5.3)]$ and $I_m = 0$ otherwise. In reality, the middle segment is modeled with both terms on the right-hand side of eq. 55, whereas the top segment is modeled with only the second term on the right-hand side. The knot occurs when $h_u = 5.3 + a(H - 5.3)$. At the knot, the value of the term $a - \frac{h_u - 5.3}{H - 5.3}$ equals 0, thus reducing eq. 55 and its derivative to only the second term on the right-hand side. The coefficients of eqs. 52, 53, and 55 for the bottom, middle, and top portions of stem, respectively, are independently estimated. This property of independence of Clark et al.'s (1991) system of taper functions likely is not a disadvantage. Instead, the independence of the equations facilitates the mathematical inversion of the equations for the computation of upper-stem height h_u and the analytical integration for volume. The ease of fitting the models and the collective performance of the taper functions over the entire profile are key factors when judging the suitability of the model.

Without question, there is a considerable art in building segmented equations. Brink and von Gadow (1983) called this a balanced compromise between the quality of the fit in a variety of complex tree shapes and the simplicity of the model. For example, Brink and von Gadow joined two differential equations at the inflection point where the stem changes from a neiloid to a paraboloid. Flewelling and Raynes (1993) introduced taper functions for western hemlock (*Tsuga heterophylla* (Raf.) Sarg.) in the US Pacific Northwest that consist of three segments and two knots with a smooth transition at the knots. These equations are complex, and a full explanation of their features and mechanics is beyond the scope of this review, yet a brief overview is provided here because of its novelty. One of the knots occurs at the height of inflection where the stem changes from a neiloid to a paraboloid (h_i), and the other knot occurs at the height where the stem changes from a paraboloid to a cone (h_c) (Fig. 11). One interesting aspect of Flewelling and Raynes' taper system is the concept of relative position of the sample tree in the diameter distribution and its importance in governing the shape of the tree. In this case, however, the diameter distribution is not stand specific, but rather determined from the pool of all destructively sampled trees. The form ratio is defined as DBH/d_{50} − 1, where d_{50} is the median value (50th percentile) of sample DBHs at a given total height. In the upper segment of the tree, stem taper is defined by a two-parameter, third-degree polynomial model:

$$(56)\qquad y = c_2 \times x + \frac{c_1}{2} \times x^2 - \frac{c_1}{6} \times x^3$$

where y is the unscaled upper-stem diameter inside bark and $x = \frac{H - h_u}{H - h_c}$. Taper in the middle segment of the tree is estimated by

$$(57)\qquad y = b_0 + b_4 \times x - \frac{b_2}{(b_1 + 1)(b_1 + 2)} \times x^{b_1 + 2} + \frac{b_2}{6} \times x^3$$

where $x = \frac{h_u - h_i}{h_c - h_i}$. Taper in the bottom segment of the tree is estimated as

$$(58)\qquad y = a_0 + \left(a_4 + \frac{a_2}{a_3}\right)x + \frac{a_2}{2a_3^2} \times x^2 + a_1 \times x^3 + a_2 \times \ln\left(1 - \frac{x}{a_3}\right)$$

where $x = \frac{h_i - h_u}{h_i}$. It should be noted that the a_i, b_i, and c_i coefficients are not directly estimated by regression. Rather, a total of eight equations involving 26 unconstrained parameters are constructed as functions of total height, DBH, and the form ratio of DBH/d_{50} − 1. Logistic transformations are made of the unconstrained functions to create shape parameters, and the a_i, b_i, and c_i coefficients are recovered from the shape parameters. Equations 56–58 produce estimates of an unscaled upper-stem diameter (y). The appropriate scaling factor (f) is computed using eq. 58 as

$$(59)\qquad f = \frac{\mathrm{DBH_{ib}}}{y_{h_u = 1.37}}$$

where $\mathrm{DBH_{ib}}$ is DBH inside bark. Upper-stem diameter is then computed as $d_u = f \times y$. Computations are not provided here on the methodology of computing the a_i, b_i, and c_i coefficients of eqs. 56–58, although it is instructive to see how the heights of the inflection knot (h_i) and the cone knot (h_c) are calculated. In this example furnished by Flewelling and Raynes (1993) in which the tree DBH is 40.15 cm and H is 24.38 m, the d_{50} of sample trees by total height is computed as $d_{50} = 4.830 \times e^{0.00651 \times H} \times (H -$

Fig. 11. Tree form based on the Flewelling and Raynes (1993) terminology: h_i is the height of the inflection point, whereas h_c is the transition height on the stem where the stem changes from a paraboloid to a cone. The taper function for the unscaled upper-stem diameter, y, in each of the three segments is a function of relative height x. The definition of relative height x changes from segment to segment. Figure was adapted from Newnham (1988).

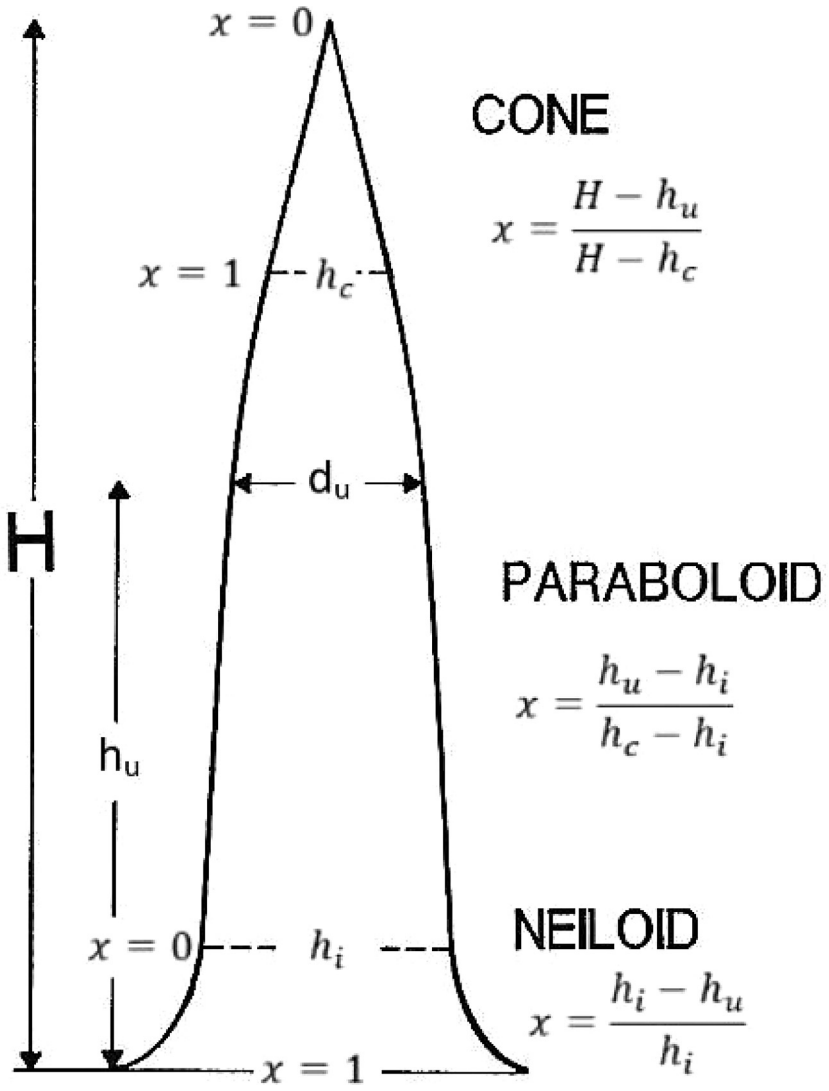

$1.37)^{0.343 + 0.005479 \times H}$ = 25.24 cm. Form ratio (fr) is computed as $\text{fr} = \frac{\text{DBH}}{d_{50}} - 1 = 0.5906$. The upper-stem height corresponding to the inflection point or knot (h_i) is $h_i = H \times \frac{e^{U_7}}{1 + e^{U_7}} = 2.93$ m, where $U_7 = -2.28 + 0.39 \times (1 - e^{-2.26 \times \text{fr}}) = -1.9927$. The upper-stem height corresponding to the knot (h_c) is $h_c = H \times \left[\frac{h_i}{H} + \left(1 - \frac{h_i}{H}\right)\frac{e^{U_8}}{1 + e^{U_8}}\right] = 21.96$ m, where $U^8 = 0.087 + 0.1903 \times H - 1.6224 \times (\text{DBH}/H)$. The Flewelling and Raynes (1993) taper functions are still widely used in the US Pacific Northwest. Although the system of equations can be integrated to compute volume, this feature is often overlooked, as transactions with roundwood and logs are largely conducted on a board-foot scale in the Pacific Northwest.

A very popular and still widely used taper function developed by Max and Burkhart (1976) models the transition from neiloid to paraboloid at the lower part of the stem and the transition from paraboloid to cone in the upper part of the stem with one smooth continuous function. The lower knot associated with the change from neiloid to paraboloid generally occurs when $h_u/H < 0.12$, which corresponds to the h_i of Flewelling and Raynes (1993). The transition from paraboloid to cone generally occurs when the knot of h_u/H exceeds 0.75%, which corresponds to the h_c of Flewelling and Raynes (1993). The Max and Burkhart (1976) taper function is expressed as

$$(60)\quad \left(\frac{d_u}{\text{DBH}}\right)^2 = b_1 \times \left(\frac{h_u}{H} - 1\right) + b_2 \times \left[\left(\frac{h_u}{H}\right)^2 - 1\right] + b_3 \times \left(a_1 - \frac{h_u}{H}\right)^2 \times I_1 + b_4 \times \left(a_2 - \frac{h_u}{H}\right)^2 \times I_2$$

where a_1 is the knot value of h_u/H or point of transition between a paraboloid and a cone in the upper part of the stem (75%–85% of

total height); a_2 is the knot value of h_u/H or point of transition between a neiloid and a paraboloid in the lower part of the stem (10%–15% of total height); $I_1 = 1$ if $h_u/H < a_1$, otherwise $I_1 = 0$; and $I_2 = 1$ if $h_u/H < a_2$, otherwise $I_2 = 0$. Because the a_i knot values are not known a priori, they must be estimated together with the b_i parameters using nonlinear regression techniques. Max and Burkhart (1976) used the technique presented by Gallant and Fuller (1973) to piece together three second-degree polynomial taper functions. The three taper functions can be expressed for the upper (eq. 61), middle (eq. 62), and bottom (eq. 63) segments, respectively, as

$$(61)\qquad \left(\frac{d_u}{\mathrm{DBH}}\right)^2_{\mathrm{upper}} = \beta_0 + \beta_1 \times \left(\frac{h_u}{H}\right) + \beta_2 \times \left(\frac{h_u}{H}\right)^2$$

$$(62)\qquad \left(\frac{d_u}{\mathrm{DBH}}\right)^2_{\mathrm{middle}} = \beta_3 + \beta_4 \times \left(\frac{h_u}{H}\right) + \beta_5 \times \left(\frac{h_u}{H}\right)^2$$

$$(63)\qquad \left(\frac{d_u}{\mathrm{DBH}}\right)^2_{\mathrm{bottom}} = \beta_6 + \beta_7 \times \left(\frac{h_u}{H}\right) + \beta_8 \times \left(\frac{h_u}{H}\right)^2$$

Max and Burkhart (1976) imposed two conditions on eqs. 61 and 62 to guarantee that at the knot value of a_1, the two functions would predict the same value of $(d_u/\mathrm{DBH})^2$ and that the transition would be smooth. The first condition requires that both functions predict the same upper-stem diameter at the knot a_1:

$$(64)\qquad \beta_0 + \beta_1 a_1 + \beta_2 a_1^2 = \beta_3 + \beta_4 a_1 + \beta_5 a_1^2$$

When the two curves join, the transition must be smooth. This is achieved if the slopes determined by the first derivatives are equal:

$$(65)\qquad \beta_1 + 2\beta_2 a_1 = \beta_4 + 2\beta_5 a_1$$

Returning to the taper function for the upper segment of the stem (eq. 61), one additional constraint was imposed, namely that $(d_u/\mathrm{DBH})^2 = 0$ when $h_u/H = 1$. This results in $\beta_0 = -\beta_1 - \beta_2$, thus producing a new taper expression for the upper segment of the stem:

$$(66)\qquad \left(\frac{d_u}{\mathrm{DBH}}\right)^2_{\mathrm{upper}} = \beta_1 \times \left(\frac{h_u}{H} - 1\right) + \beta_2 \times \left[\left(\frac{h_u}{H}\right)^2 - 1\right]$$

Isolating the β_4 term of eq. 65 produces $\beta_4 = \beta_1 + 2\beta_2 a_1 - 2\beta_5 a_1$. Inserting the expressions for β_0 and β_4 into eq. 64 provides a new function for β_3: $\beta_3 = -\beta_1 - \beta_2 - \beta_2 a_1^2 + \beta_5 a_1^2$. Inserting this expression for β_3 and the previous value of β_4 into eq. 62, it is now possible to rewrite the expression for the middle segment:

$$(67)\qquad \left(\frac{d_u}{\mathrm{DBH}}\right)^2_{\mathrm{middle}} = -\beta_1 - \beta_2 - \beta_2 a_1^2 + \beta_5 a_1^2 + (\beta_1 + 2\beta_2 a_1 - 2\beta_5 a_1) \times \left(\frac{h_u}{H}\right) + \beta_5 \times \left(\frac{h_u}{H}\right)^2$$

The key at this point is to both add and subtract $\beta_2 \times (h_u/\mathrm{H})^2$ to eq. 67. Now it is possible to express the middle segment taper as

$$(68)\qquad \left(\frac{d_u}{\mathrm{DBH}}\right)^2_{\mathrm{middle}} = \left(\frac{d_u}{\mathrm{DBH}}\right)^2_{\mathrm{upper}} + (\beta_5 - \beta_2) \times \left[a_1^2 - 2a_1\left(\frac{h_u}{H}\right) + \left(\frac{h_u}{H}\right)^2\right]$$

With the addition of an indicator variable, I_1, and reparameterizing β_1, β_2, and $(\beta_5 - \beta_2)$ as b_1, b_2, and b_3, respectively, it is possible to use one expression to model the stem profile of the middle and upper segments of the tree:

$$(69)\qquad \left(\frac{d_u}{\mathrm{DBH}}\right)^2 = b_1 \times \left(\frac{h_u}{H} - 1\right) + b_2 \times \left[\left(\frac{h_u}{H}\right)^2 - 1\right] + b_3 \times \left(a_1 - \frac{h_u}{H}\right)^2 \times I_1$$

where $I_1 = 1$ if $h_u/H < a_1$, otherwise $I_1 = 0$. The same procedure can be used for splining the lower segment of the tree with the middle segment equation (eq. 69) at the knot value of a_2. The Max and Burkhart (1976) taper function has been applied to major forest species in both the Northern and Southern Hemispheres and still has wide acceptance. Martin (1981) has demonstrated how eq. 60 can be inverted to predict h_u as a function of d_u. In addition, Martin furnished an analytical integrated solution for volume. Nonlinear regression techniques must be used to estimate the parameters, and occasionally it can be difficult to obtain convergence or significant coefficients for the knots a_1 and a_2. This drawback can be easily surmounted by fitting eq. 60 with a linear model inside a loop and using an array of predetermined values for a_1 and a_2 in the suggested ranges of $0.75 \le a_1 \le 0.85$ and $0.10 \le a_2 \le 0.15$.

The Max and Burkhart (1976) taper model contains three segments, two knots, and five restrictions or constraints. There is a flexible and less tedious methodology for adding additional segments and knots for splined polynomial taper functions. Unlike B-splines, the methodology here displays stable behavior before the first knot and after the last knot. This methodology maintains the smoothness at the knots with equal values of the first derivative for the two segments at the knot. Following a technique by Pedan (2003), Scolforo et al. (2018) employed quadratic polynomials with $K = 4$ empirical knots ($k_1 = 0.10$, $k_2 = 0.34$, $k_3 = 0.75$, and $k_4 = 0.97$). In addition, these authors also added a tree size variable (S) to the model form:

$$(70)\qquad \frac{d_u}{\mathrm{DBH}} = b_1 \times \left(1 - \frac{h_u}{H}\right) + b_2 \times \left(1 - \frac{h_u}{H}\right)^2 + b_3 \times S + \sum_{k=1}^{K} u_k \times \left[\left(1 - \frac{h_u}{H}\right) - k_1\right]_+^2$$

where b_1–b_3 are the coefficients to be estimated; $S = \frac{\mathrm{DBH}^2 \times H}{10\,000} \times \ln\left(2 - \frac{h_u}{H}\right)$; u_k are the knot variable coefficients to be estimated; and the subscript operator "+" infers that the function is only computed if $1 - (h_u/H)$ is larger than the knot value inside the parentheses, otherwise the value is zero. Hence, this value replaces the indicator variable used in the Max and Burkhart (1976) taper function with greater implied flexibility. Equation 71, defined by Scolforo et al. (2018) as the penalized mixed spline (PMS) approach, is a normal linear mixed-effects model, in which the quadratic expression and S are fixed and the expressions for the knots are declared random based on each tree (stand) and stand. It is suggested that the mixed-effects model then resolves the smoothing spline regression, which turns it into a penalized regression spline (Pedan 2003):

$$(71)\qquad y = \mathbf{X}b + \mathbf{Z}u + \varepsilon,\ [u, \varepsilon]^T \sim N\left(0, \mathrm{diag}\left(\sigma_u^2 I, \sigma_\varepsilon^2 I\right)\right)$$

where

$$\mathbf{X} = \begin{bmatrix} \left(1-\frac{h_1}{H_1}\right) & \left(1-\frac{h_1}{H_1}\right)^2 & \mathrm{DBH}^2 H \ln\left(2-\frac{h_1}{H_1}\right) \\ \vdots & \vdots & \vdots \\ \left(1-\frac{h_n}{H_n}\right) & \left(1-\frac{h_n}{H_n}\right)^2 & \mathrm{DBH}^2 H \ln\left(2-\frac{h_n}{H_n}\right) \end{bmatrix}$$

$$\mathbf{Z} = \begin{bmatrix} \left[\left(1-\frac{h_1}{H_1}\right)-k_1\right]_+^2 & \cdots & \left[\left(1-\frac{h_1}{H_1}\right)-k_k\right]_+^2 \\ \vdots & \vdots & \vdots \\ \left[\left(1-\frac{h_n}{H_n}\right)-k_1\right]_+^2 & \cdots & \left[\left(1-\frac{h_n}{H_n}\right)-k_k\right]_+^2 \end{bmatrix}$$

Mixed model application also makes it quite easy to account for the autocorrelation within the stem of measurements at each bolt cut. The locations of the knots in the PMS model are predetermined. Harrell (2015) suggested the addition of more knots to a model as an adequate trade-off to determining the exact point of transition between segments. However, it is important to be prudent and terminate the addition of additional knots at the point at which the u_k coefficients are no longer statistically significant.

Polynomials, segmented models, and splined taper functions are among the oldest of the modern taper model forms and have a long history of development and use but present some challenges in their proper formulation and parameterization. This may have limited their development and application in more recent decades.

2.3.4. *Trigonometric models and matrix functions*

Taper equations with trigonometric functions have a particular appeal when modeling the profile of species that has a pronounced flare in the bottom portion of the tree. They are often similar to the variable-form taper equations previously discussed but can be simpler in their formulation given the reliance on multiple trigonometric functions. With their inverse sigmoid shape, they can match the stump swell at the ground line and the remainder of the stem with only a few parameters. Matney et al. (1985) proposed the following model of relative height for several southern US hardwood species:

$$\frac{h_u}{H} = 1 - \left\{1 - e^{-a \times \tan[b \times H^c \times (d_u/\mathrm{DBH})]}\right\}^d \quad (72)$$

where b, c, and d are parameters to be estimated and tan is the tangent measured in radians. The parameter a may be isolated and conditioned to predict that h_u = 1.3 when d_u = DBH: $a = \frac{-\ln\left\{1-[1-(1.3/H)]^{1/d}\right\}}{\tan(b \times H^c)}$. Equation 72 may be inverted to predict d_u as a function of h_u. Thomas and Parresol (1991) used sine and cotangent variables to obtain profile flexibility with only three parameters:

$$\left(\frac{d_u}{\mathrm{DBH}}\right)^2 = a_1 \times \left(\frac{h_u}{H}-1\right) + a_2 \times \left[\sin\left(c \times \pi \times \frac{h_u}{H}\right)\right] + a_3 \times \left[\cot\left(\frac{\pi \times \frac{h_u}{H}}{2}\right)\right] \quad (73)$$

where c = 1.5 for slash pine and 2.0 for willow oak (*Quercus phellos* L.). Likewise, Bi (2000) used trigonometric functions and a formulation resembling the Kozak (1988) and Newnham (1988) models to arrive at a flexible taper function that is relatively easy to fit:

$$\frac{d_{u(ib)}}{\mathrm{DBH}_{(ib)}} = B^K \quad (74)$$

where

$$B = \frac{\ln\left[\sin\left(\frac{\pi}{2} \times \frac{h_u}{H}\right)\right]}{\ln\left[\sin\left(\frac{\pi}{2} \times \frac{1.3}{H}\right)\right]}$$

and

$$K = a_1 + a_2 \times \sin\left(\frac{\pi}{2} \times \frac{h_u}{H}\right) + a_3 \times \cos\left(\frac{3\pi}{2} \times \frac{h_u}{H}\right) + a_4 \times \frac{\sin\left(\frac{\pi}{2} \times \frac{h_u}{H}\right)}{\frac{h_u}{H}} + a_5 \times \mathrm{DBH} + a_6 \times \frac{h_u}{H} \times \sqrt{\mathrm{DBH}} + a_7 \times \frac{h_u}{H} \times \sqrt{H}$$

Similar to the Kozak (1988) and Newnham (1988) taper models, upper-stem height (h_u) and volume must be computed by inverting eq. 74 using numerical techniques.

Kilkki et al. (1978) introduced a completely different methodology of inspecting tree taper using matrix algebra for Scots pine (*Pinus sylvestris* L.) in Finland, which was called a simultaneous equation model. The premise was that each upper-stem diameter can be predicted by an equation in which all other observed upper-stem diameters are predictors. Additional variables indicating tree size such as total height are also included in the prediction equation. For the sake of brevity, this concept will be presented using only four upper-stem measurements. Ideally, however, this application would have 10 or more upper-stem diameter measurements, presumably wherever there is a bolt cut. The bolt cuts of the destructively sampled tree should not be a fixed length apart, rather the tree should be sectioned in 10 or more sections of equal relative length. The Kilkki et al. (1978) premise is re-created here with four simultaneous equations:

$$\begin{aligned} 0 + a_{12} \times d_{u2} + a_{13} \times d_{u3} + a_{14} \times d_{u4} + k_1 &= d_{u1} \\ a_{21} \times d_{u1} + 0 + a_{23} \times d_{u3} + a_{24} \times d_{u4} + k_2 &= d_{u2} \\ a_{31} \times d_{u1} + a_{32} \times d_{u2} + 0 + a_{34} \times d_{u4} + k_3 &= d_{u3} \\ a_{41} \times d_{u1} + a_{42} \times d_{u2} + a_{43} \times d_{u3} + 0 + k_4 &= d_{u4} \end{aligned} \quad (75)$$

The a_{ij} coefficients are estimated by regression for each d_{ui} with independent models. The k_i variables represent tree size, as a function of total height, and are expressed as

$$k_i = k_{0i} + k_{1i} H + k_{2i} H^2 \quad (76)$$

where H is total tree height and k_0, k_1, and k_2 are regression parameters. With some rearrangement of the terms, eq. 75 is expressed as

$$\begin{aligned} -1 \times d_{u1} + a_{12} \times d_{u2} + a_{13} \times d_{u3} + a_{14} \times d_{u4} &= -k_1 \\ a_{21} \times d_{u1} - 1 \times d_{u2} + a_{23} \times d_{u3} + a_{24} \times d_{u4} &= -k_2 \\ a_{31} \times d_{u1} + a_{32} \times d_{u2} - 1 \times d_{u3} + a_{34} \times d_{u4} &= -k_3 \\ a_{41} \times d_{u1} + a_{42} \times d_{u2} + a_{43} \times d_{u3} - 1 \times d_{u4} &= -k_4 \end{aligned} \quad (77)$$

A detached coefficient matrix notation may be used to represent the system $\mathbf{A}\boldsymbol{x} = \boldsymbol{b}$:

$$\begin{bmatrix} -1 & \alpha_{12} & \alpha_{13} & \alpha_{14} \\ \alpha_{21} & -1 & \alpha_{23} & \alpha_{24} \\ \alpha_{31} & \alpha_{32} & -1 & \alpha_{34} \\ \alpha_{41} & \alpha_{42} & \alpha_{43} & -1 \end{bmatrix} \begin{bmatrix} d_{u1} \\ d_{u2} \\ d_{u3} \\ d_{u4} \end{bmatrix} = \begin{bmatrix} -k_1 \\ -k_2 \\ -k_3 \\ -k_4 \end{bmatrix} \quad (78)$$

The solution is then $\boldsymbol{x} = \mathbf{A}^{-1}\boldsymbol{b}$, where the $\boldsymbol{x}$ vector contains the upper-stem diameters d_{ui} and $\mathbf{A}^{-1}$ is the inverted matrix of the a_{ij} coefficients with –1 on the diagonal. Interpolation must be used

Fig. 12. The matrix approach of Kilkki et al. (1978) provides a smooth transition at the knots formed by the intersection of h_{ui} and d_{ui}. At the first and last segment, b_1 and b_3 may be estimated from b_2. The key relationships are $f_1 = d_{u1} - \frac{d_{u2} - d_{u1}}{h_{u2} - h_{u1}} h_{u1} + \frac{d_{u2} - d_{u1}}{h_{u2} - h_{u1}} h_u = a_1 + b_1 h_u$, $f_2 = d_{u2} - \frac{d_{u3} - d_{u2}}{h_{u3} - h_{u2}} h_{u2} + \frac{d_{u3} - d_{u2}}{h_{u3} - h_{u2}} h_u = a_2 + b_2 h_u$, and $f_3 = d_{u3} - \frac{d_{u4} - d_{u3}}{h_{u4} - h_{u3}} h_{u3} + \frac{d_{u4} - d_{u3}}{h_{u4} - h_{u3}} h_u = a_3 + b_3 h_u$. Figure was adapted from Kilkki et al. (1978).

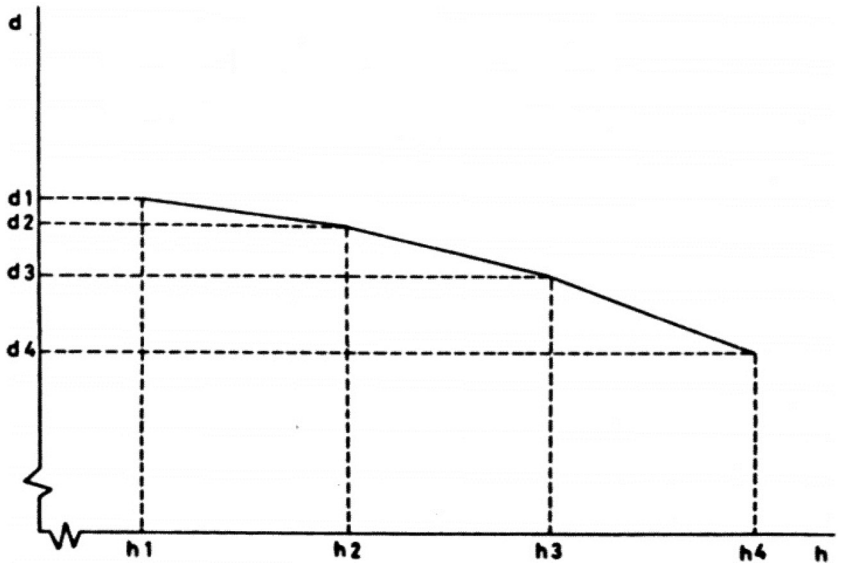

to estimate the upper-stem diameter between the diameters d_{ui}. Kilkki et al. (1978) presented a rather sophisticated interpolation rule that ensures a monotonic decrease in upper-stem diameter between predicted d_{ui} values:

$$d_u = f_2 + (f_1 - f_2) \times \frac{|b_2|}{|b_1| + |b_2|} \times \left(\frac{h_{u3} - h_u}{h_{u3} - h_{u2}} \right)^{2.4} + (f_3 - f_2) \times \frac{|b_2|}{|b_2| + |b_3|} \times \left(\frac{h_u - h_{u2}}{h_{u3} - h_{u2}} \right)^{2.4} \quad (79)$$

where $h_{u2} \le h_u \le h_{u3}$ and $d_{u2} \le d_u \le d_{u3}$. The f_i and b_i values are explained in Fig. 12. It is hardly surprising that the regression fits are outstanding for the system represented by eq. 75, given the number of variables used to estimate d_{ui}. Clearly, however, the equations are not independent, and users of this method should consider the use of two- or three-stage least squares methods for estimating the system of equations.

Trigonometric models and matrix functions are a special class of taper equations that offer some relative simplicity for addressing species with complex stem forms. Trigonometric models share many similarities to variable-form approaches with high flexibility, ease of parameterization, and robust accuracy. Beyond Kilkki et al. (1978), matrix functions have seen more limited application but could offer significant advantages if multiple upper-stem diameters have greater availability in the future, perhaps with terrestrial laser scanning (see section 5).

2.4. Inclusion of additional model covariates

Nearly all of the taper equations previously shown are primarily a function of relative height in the stem, DBH, and H, as these are the most common variables taken in routine inventories. Moreover, there have been a number of attempts to improve taper equation performance by incorporating additional model covariates, including (*i*) upper-stem diameter measurements, (*ii*) crown size variables, (*iii*) tree form classifications, and (*iv*) stand- or site-level factors.

2.4.1. Upper-stem diameters

As noted by Goodwin (2009), a key limitation of relying primarily on DBH is that the volume of small trees cannot be determined and breast height might not be the most optimal location for predicting stem form. Goodwin noted that relative heights between 10% and 30% provided much better estimates of tree form than DBH, consistent with the tendency to include additional upper-stem diameter measurements as predictors (Clark et al. 1991; Kozak 1998; Jordan et al. 2005). As well summarized by Sabatia and Burkhart (2015), the recommended optimal location of this upper-stem diameter measurement has varied considerably and likely depends on the species, the specific taper equation being used, and the ability to measure upper-stem diameter measurements accurately. For example, fixed heights of 5–9 m have been suggested as optimal (Clark et al. 1991; Trincado and Burkhart 2006; Yang et al. 2009; Gómez-García et al. 2013), whereas relative heights of 30%–40% (Sharma and Zhang 2004; Sharma and Parton 2009), 40%–50% (Kozak 1998), and values > 50% (Cao 2009; Sabatia and Burkhart 2015) have also been suggested.

Although these measurements can be helpful in improving predictive performance, measuring upper-stem diameter on standing trees can be difficult, as evidenced by Westfall et al. (2016) who indicated that measurement error increases with tree size, differs across species and measurement devices, and needs to be within ±0.2 cm to ensure proper prediction accuracy, which generally questions the robustness of most field-based assessments of upper-stem diameter. Likewise, imputation of upper-stem diameter using a model (e.g., Clark et al. 1991) can also have unintended consequences for the general usefulness of this variable as a predictor as showcased by Li and Weiskittel (2010).

2.4.2. Crown size

The influence of crown length on stem form has long been recognized (Pressler 1864; Larson 1963), yet its inclusion in taper equations has varied. For example, some studies have found them to be nonsignificant or to only marginally improve model fits (Burkhart and Walton 1985; Muhairwe et al. 1994; Li and Weiskittel 2010), whereas other studies (Hann et al. 1987; Leites and Robinson 2004; Yang et al. 2009) have found otherwise, suggesting that it might depend on the available data, species, and model form. As noted by Weiskittel et al. (2011), the inclusion of crown variables might not be to just simply improve model fit predictions, but to ensure more logical biological behavior. A taper equation should predict trees with shorter crowns compared with similar-sized trees with larger crowns to have (*i*) wider diameters above DBH, (*ii*) narrower diameters below DBH, and (*iii*) a similar DBH. Consequently, the continual exploration of including crown variables is still important and encouraged. This can include the further testing of crown variables across a broader range of species and stand conditions, as well as the influence of various measures of crown. For example, crown ratio has been commonly used, whereas height to crown midpoint (Dean et al. 2002), crown length (Özçelik and Bal 2013), crown ratio weighted DBH (MacFarlane 2010), or a combination of crown variables might be more effective (Leites and Robinson 2004).

2.4.3. Tree class and form classification

Trees have been known to vary in their form and its related influence on volume with the relative wide use of form classes; however, the use of tree form has had more limited use in stem taper equations. This might simply be a function of taper studies that focus only on trees with some idealized stem form, particularly in broad-leaved species, or more general species that rarely have a continuous stem (MacFarlane and Weiskittel 2016). When trees from diverse morphological types were tested with a large data set without any exclusion criteria, it was found that a simple tree form classification system explained the most variation between trees and stands, even across species (MacFarlane and Weiskittel 2016). In this analysis, the tree form classification was based on a merchantable form type, which focused on whether or not the tree contained merchantable wood in some or all of the following four categories: (*i*) main stem pulpwood, (*ii*) main stem sawtimber, (*iii*) branch pulpwood, or (*iv*) branch sawtimber (MacFarlane and Weiskittel 2016). Given its generality, extension of this approach to other species and regions is logical.

Likewise, Castle et al. (2017) found that hardwood stem form was strongly influenced by a more involved yet generic stem form and risk classification of Pelletier et al. (2014), which should be further explored across a broader array of species and stand or site conditions. Rather than using form class, Sanquetta et al. (2020) found the widely used tree hierarchical position classification (e.g., dominant and intermediate) to be influential.

2.4.4. Stand- and site-level factors

Because of stand- and site-level influences on both *H*–DBH and crown size relationships, a strong influence is expected on stem form and volume. However, a more limited set of studies has examined these relationships beyond the studies previously described (e.g., Muhairwe et al. 1994; Madsen 1985), and this might be an important area for future research. Early research by Muhairwe et al. (1994) found that site class and stand age were not influential predictors of stem form, likely because their effect is implicitly captured by the use of both DBH and *H* in most taper equations. Subsequent research has highlighted the potential effect of stand age (Liu et al. 2020*b*) and stand density even after the inclusion of DBH and *H* (Sharma and Zhang 2004; Sharma and Parton 2009; Duan et al. 2016).

Although these studies have found an influence of stand density on stem taper, they have been primarily focused on stem number per hectare and not other more sophisticated measures of stand density, which appears like a logical area of future exploration and has shown greater predictive power (Schneider 2019). As previously noted, Brink and von Gadow (1983) used stand-level quadratic mean diameter as an important predictor of stem taper, whereas Liu et al. (2020*b*) and Sanquetta et al. (2020) used a measure of relative stocking and relative spacing index, respectively. Likewise, Sharma (2020) found that the square root of the ratio of stand basal area to stem number was the best stand density predictor for a single softwood species in Canada. Recently, Poudel et al. (2020) indicated significant differences in stem form based on trees from different stand origins (i.e., natural, plantation, and coppice), and this might be an important stand-level factor in regions with mixed regeneration strategies similar to the findings of Li et al. (2012) (Fig. 6).

At the site level, focus has primarily been on the use of ecoregions (Huang et al. 2000; Kozak 2004; Özçelik et al. 2016; López-Martínez et al. 2020) and climate (Nigh and Smith 2012; Schneider et al. 2018; Schneider 2019; Liu et al. 2020*a*). For example, Huang et al. (2000) found significant differences in stem taper across five of the seven ecoregions tested in Alberta, Canada, that reduced mean squared error (MSE) up to 50%, and Schneider et al. (2018) observed climate-induced changes in stem form in four of the five boreal species they examined, with up to 5% difference in stem volume related to climate. These climate-related changes were found to significantly interact with tree species functional traits like shade tolerance (Schneider et al. 2018), which highlights an area for future research. Also, as recently highlighted by Schneider (2019), the role of wind as originally noted by Metzger (1893) (see section 2.1) could be particularly important in areas with high exposure and deserves further evaluation given the better availability of high-resolution mean wind speed data. Overall, the use of ecoregion and climate appears justified in the development of broad-scale equations, especially for species that cover a large range of conditions.

3. Model parameterization

Three primary regression approaches have been used to derive taper equations: (*i*) parametric, (*ii*) semiparametric, and (*iii*) nonparametric. All have distinct advantages and disadvantages (Table 2).

3.1. Parametric

The vast majority of taper model forms are parametric fitted by purely parametric methods like ordinary least squares (OLS) (e.g., Kozak et al. 1969), nonlinear least squares (NLS) (e.g., Goodwin 2009), seemingly unrelated regression (SUR) (e.g., Jordan et al. 2005), three-stage least squares (e.g., Zakrzewski and MacFarlane 2006), quantile regression (Cao and Wang 2015; Özçelik et al. 2019), and most recently, stochastic differential equations (Narmontas et al. 2020). In the last decade, the use of nonlinear mixed-effects modeling (NLME) has become the dominant form of fitting stem taper equations (e.g., Li et al. 2012; MacFarlane and Weiskittel 2016; Scolforo et al. 2018), which was first introduced for stem taper modeling by Gregoire and Schabenberger (1996). Mixed models provide a flexible framework for properly accounting for the nested or hierarchical nature of most stem taper data sets while providing a direct benefit of allowing for local calibration (e.g., Trincado and Burkhart 2006), which is further discussed in section 4.2.

In addition to being hierarchical in nature, stem taper models can have high multicollinearity, autocorrelation, and heteroskedasticity, which each rely on distinct statistical methods for effectively addressing them. Kozak (1997) examined the effects of multicollinearity and autocorrelation on stem taper predictive performance and found that equations generally remained unbiased yet had much greater variability when severe multicollinearity was present. As previously discussed, this is often why selection of the proper taper model form is more important than

Table 2. Overview of the primary parametric, semiparametric, and nonparametric stem taper methods with advantages, disadvantages, and examples identified.

Parameterization method	Advantages	Disadvantages	Example(s)
Parametric			
Ordinary least squares (OLS)	Robust and provides unbiased parameter estimates; starting values are not needed; fast convergence	Does not accommodate hierarchical data; limited to linear model forms; requires meeting numerous assumptions	Kozak et al. (1969); Téo et al. (2018)
Nonlinear mixed-effects (NLME)	Accommodates complex hierarchical data; easily allows for local calibration; can provide improved parameter estimates and their uncertainty	Proper convergence can be a challenge or time intensive for large data or complex model forms; requires robust starting values	Garber and Maguire (2003); Gregoire and Schabenberger (1996); Li and Weiskittel (2010)
System of equations	Accommodates multiple equations as a system and effectively addresses cross-equation correlations	Potential limited gains in predictive accuracy; may constrain most optimal parameter estimates	Three-stage least squares (Zakrzewski and MacFarlane 2006); seemingly unrelated regression (SUR) (Fang et al. (2000); Jordan et al. (2005))
Semiparametric			
Generalized additive models (GAMs)	High flexibility; incorporation of random effects; widely available in statistical software	Potential for overfitting; lose precision when smoothing terms are outside the training range	Robinson et al. (2011); Marchi et al. (2020)
B- and P-splines	High flexibility; incorporation of random effects; robust performance; can be constrained	Complex and may overfit; need robust training data sets	Kublin et al. (2008, 2013); Kuželka and Marušák (2014*a*, 2014*b*)
Penalized mixed splines (PMS)	High flexibility; incorporation of random effects; robust performance; relative ease of fitting	Potential for overfitting; need robust training data sets	Scolforo et al. (2018)
Nonparametric			
Random forest	Uses cross-validation methods to avoid overfitting; robust algorithm with strong predictive performance	Need extensive and representative training data sets; cannot extrapolate beyond training data; algorithms may need to be modified to accommodate hierarchical data; limited portability to other users	Nunes and Görgens (2016); Yang and Burkhart (2020)
Artificial neural network (ANN)	Uses cross-validation methods to avoid overfitting; highly tunable		Ozçelik et al. (2010); Socha et al. (2020)

the actual fitting method. Similar to OLS or NLS, mixed models do allow for effective handling of both autocorrelation and heteroskedasticity. Garber and Maguire (2003) noted that the inclusion of tree-level random effects reduced some of the within-tree autocorrelation, but first-order continuous autoregressive (CAR1) error structure was needed to remove it completely, which has been further supported in other studies (Trincado and Burkhart 2006; Li et al. 2012). Weighting has long been a topic of focus in stem taper modeling with varied findings (Cormier et al. 1992). Currently, most stem taper equations employ an optimized variance power weighting as a function of the relative height in the stem (Garber and Maguire 2003; Li et al. 2012; Scolforo et al. 2018), which has been found to significantly improve model performance.

Although most stem taper equations are unbiased and relatively accurate predictors of tree volume (Li and Weiskittel 2010), they are optimized to predict stem diameter rather than stem volume. As previously described, this is one of the stated benefits of the compatible stem taper and volume equations, which could be estimated using SUR (e.g., Jordan et al. 2005) or three-stage least squares (Zakrzewski and MacFarlane 2006). Gains in accuracy are not always evident and might compromise predictions of both stem diameter and volume. Li and Weiskittel (2010) found that a compatible prediction system was one of the lowest ranking for both stem diameter and volume when compared with 10 other noncompatible stem taper equations (Table 3), whereas other recent studies have found otherwise (e.g., Shahzad et al. 2020), suggesting that it might differ by species.

Table 3. Median ranking of various stem taper equations in terms of predictions of stem diameter and total volume based on various model fit statistics across three softwood species in Maine, United States.

	Median rank		
Equation	Stem diameter	Total stem volume	Overall
Max and Burkhart (1976)	6	11	8.5
Kozak (2004) Model 01	11	7	9
Kozak (2004) Model 02	1	4	2.5
Bi (2000)	2	3	2.5
Zakrzewski (1999)	5	5	5
Valentine and Gregoire (2001)	3	2	2.5
Sharma and Zhang (2004)	7	8	7.5
Sharma and Parton (2009)	8	10	9
Clark et al. (1991) I[a]	5	1	3
Clark et al. (1991) II[b]	10	9	10
Fang et al. (2000)	7	6	6.5

Note: Based on data presented by Li and Weiskittel (2010).
[a]Used observed upper-stem diameter at 5.3 m.
[b]Used predicted upper-stem diameter at 5.3 m.

Instead of focusing on compatibility, several authors have begun exploring alternative optimization algorithms to improve parameter estimation for stem taper equations. Pang et al. (2016) found that a combined method of constrained two-dimensional

Table 4. Examples of stem taper equation use across various organizations and agencies throughout North America.

Organization	Equation(s)	Reference
Canadian Forest Service	Modified Sharma and Oderwald (2001) fit with or without measured total height	Ung et al. (2013)
New Brunswick Department of Natural Resources and Energy Development	Modified Kozak (2004) for primary softwood and hardwood species	Li et al. (2012)
Quebec Ministry of Forests, Wildlife and Parks	Modified Sharma and Oderwald (2001) for nine species	Schneider et al. (2013)
US Forest Service, Forest Inventory and Analysis	Modified Valentine and Gregoire (2001) model form for 19 species groups in the northeastern US	Westfall and Scott (2010)
US Forest Service, National Forest	Depends on region, but includes use of Clark et al. (1991), Flewelling and Raynes (1993), Wensel and Olson (1995), and many others	National Volume Estimator Library (NVEL; https://www.fs.fed.us/forestmanagement/products/measurement/volume/nvel/index.php)

optimum seeking and least square regression outperformed traditional OLS for stem taper equations for three tropical species in China, and Nicoletti et al. (2020) used bivariate modeling for modeling stem taper for loblolly pine in Brazil. Özçelik and Cao (2017) suggested that optimizing for both taper and either cumulative or total volume performed better than other methods.

3.2. Semiparametric

Semiparametric methods like splines have been extensively used for modeling stem taper (Lappi 2006; Kublin et al. 2008; Scolforo et al. 2018). The splining methodology has varied and has included the use of smoothing splines (Lappi 2006), generalized additive models (GAMs) (Robinson et al. 2011; Marchi et al. 2020), B-splines (Kublin et al. 2008, 2013), P-splines (Kuželka and Marušák 2014*a*), and penalized mixed splines (PMS) (Scolforo et al. 2018). Several additional forms of splines were explored by Kuželka and Marušák (2014*b*), who suggested that interpolation curves with first-degree continuity determined by the Catmull and Rom (1974) spline performed best. Splines offer greater flexibility in the fit without a greater addition of fixed parameters, which may enhance representation on stem form variability commonly seen in some species, especially hardwoods or softwoods with significant stump flare.

Semiparametric methods can also include a random effect similar to the mixed models previously described, which allows for better localization (Kublin et al. 2008). In comparison with more traditional methods, performance of semiparametric methods has varied. For example, Scolforo et al. (2018) found that a generalized PMS approach gave more stable volume predictions, particularly across tree size classes. This is consistent with the finding of Kuželka and Marušák (2014*a*), who found P-splines to be superior to other widely used parametric model forms. Likewise, both Robinson et al. (2011) and Marchi et al. (2020) found that GAMs generally outperformed parametric methods, but the degree of improvement did vary by species.

Although semiparametric methods do offer greater flexibility and predictive performance, two potential drawbacks are overfitting and a decrease of model portability. Kuželka and Marušák (2014*b*) clearly demonstrated that spline predictive performance was very sensitive to the number of input points (knots) and order (e.g., second vs. third order). Fitting of semiparametric methods is relatively straightforward using the approaches previously outlined or in R with the TapeR package (Kublin and Breidenbach 2013). Likely, the best use of semiparametric methods for taper equation development are when localized predictions are needed.

3.3. Nonparametric

Similar to semiparametric methods, fully nonparametric methods have seen wider use for taper predictions. This has included the use of regression trees or forests (Nunes and Görgens 2016; Yang and Burkhart 2020) and artificial neural networks (Özçelik et al. 2010; Socha et al. 2020). The random forest algorithm is commonly used for regression trees, whereas various algorithms are available for neural networks and can give different results (Özçelik et al. 2010). Comparing these methods, neural networks have been shown to generally outperform regression trees, which both tend to outperform parametric methods (Nunes and Görgens 2016). However, unlike mixed models, nonparametric methods do not tend to address hierarchies in the data, which are generally quite prevalent in taper data sets. To address this, two-stage bootstrapping approaches or hierarchical random forest methods must be used. Recently, Yang and Burkhart (2020) found that the comparisons between parametric and nonparametric methods depended heavily on the underlying verification data with nonparametric methods being more sensitive.

Like semiparametric approaches, nonparametric methods offer several advantages that deserve additional exploration. Notably, there are also some important drawbacks, which include (*i*) the need for a highly representative and extensive database, as the methods cannot predict outside of the range of the training data; (*ii*) they can overfit the data and give biologically implausible predictions; (*iii*) reduced portability to other users; and (*iv*) the predictions are nontractable in terms of both estimation and quantification of uncertainty that would require numerical integration to derive volume. Similar to semiparametric methods, nonparametric methods might be best when local predictions are needed or for species with complex form types assuming that extensive data are available.

4. Development, application, and use

Despite their general complexity, stem taper equations are meant to be developed and used for a variety of practical and scientific applications (Table 4). As previously described, a range of taper model formulations and methods of parameter estimation are currently in use (Table 2); this variety can make development a challenge and highly dependent on sample size, measurement methods, and tree selection protocols. With the wide use of mixed-effect models, local calibration using a few upper-stem diameter measurements is now possible and can prevent the need to develop new equations. For effective application, users need to potentially consider numerical integration methods, as well as bolt length, the conversion between inside- and outside-bark diameters, and imputation of missing values like total height. Each of these issues is briefly elaborated on in the following sections.

4.1. Sample size and tree selection

Stem taper equations require multiple observations of inside- and outside-bark diameters, which can be taken on standing or destructively sampled trees. Given the challenges of measuring upper-stem diameters (Westfall et al. 2016) and the larger interest in

inside-bark diameter, taper measurements from felled trees are generally preferred and have long been the primary means for a variety of applications (Behre et al. 1926). Important considerations in collecting the necessary data to develop a taper equation are (*i*) number of sample trees; (*ii*) selection of sample trees; and (*iii*) number, arrangement (e.g., equidistant vs. relative), and location of diameter measurements along the stem.

Various factors such as species, model form, and expected range of tree DBHs desired for application influence the optimal tree sample size number estimate (Subedi et al. 2011). Kitikidou and Chatzilazarou (2008) found that at least 825 observations of stem diameters along the bole were needed to properly parameterize a taper equation. If 10–20 observations were taken from each sample tree, then a minimum of 40–85 sample trees would be needed, which is consistent with recommendations from prior analyses (Kitikidou and Chatzilazarou 2008; Subedi et al. 2011; Stängle et al. 2016; Saarinen et al. 2019). However, there is often a significant interaction between sample size and tree selection criteria. Subedi et al. (2011) found that stratified random sampling by selecting across a range of diameter classes was most efficient when compared with other methods. At the very least, selecting trees near the minimum and maximum of the DBH range where the equation will be used is important, particularly if nonparametric parameterization will be used.

Most volume and biomass studies sample trees well below the largest tree DBH in an inventory because of the time, expense, and value of measuring larger trees (Frank et al. 2019). In addition, most taper studies likely do not utilize a fully random selection methodology; often, vigorous and well-formed trees free of defect are selected and used. Such selectivity can have important implications for the representativeness of the developed equation (MacFarlane and Weiskittel 2016), as a significant fraction of the underlying regional forest inventory may not fit these properties, especially in areas dominated by hardwoods (Castle et al. 2018).

Within a tree, either relative or absolute methods are often used to select locations for measuring diameters. For example, Westfall and Scott (2010) used measurements at 0.3, 0.6, 0.9, 1.4, and 1.8 m and approximately every 1–2.5 m to tree tip to develop stem taper equations for a variety of species in the northeastern US, and Laasasenaho et al. (2005) used observations collected at 1%, 2.5%, 5%, 7.5%, 10%, 15%, 20%, 30%, 40%, 50%, 60%, 70%, 80%, and 90% of total tree height for their stem taper equations. Often, the highest variation and change in stem form is near the tree base, and additional measurements are generally taken to effectively capture it, particularly if predictions below 1.3 m are needed. At minimum, measurements should be taken at least every 2 m (e.g., Stängle et al. 2016), as bias can occur if volume is estimated with longer intervals (Filho and Schaaf 1999). Further, perpendicular measurements of major or minor axes of both diameter inside and outside bark are generally needed to capture variation, and the use of bark thickness gauges can result in significant bias (e.g., Stängle et al. 2016).

4.2. Calibration

Calibration can be achieved with different means and often requires a much smaller sample size than developing a new stem taper equation. A clear advantage of using mixed-effect models is the ability to estimate a random effect from a small number of samples (Trincado and Burkhart 2006), which has generally been shown to outperform other calibration methods (Cao and Wang 2011, 2015). As previously discussed, the number, location, and type (inside vs. outside bark) of observations can control the effectiveness of local calibration. For example, Cao (2009) found that a diameter measurement at the midpoint between breast height and the tree tip significantly and modestly improved predictions of outside and inside bark, respectively. One important drawback to mixed-effects calibration methods is that they often require the full error structure of the original fit model to be available, which is rarely the case. It would be useful if authors might consider publishing these as supplemental files in future studies.

In addition, because of the common lack of upper-stem diameter measurements, de-Miguel et al. (2012) proposed three alternative strategies for calibration and suggested that computing mean predictions from a mixed-effects model over the distribution of random effects was the best approach. Likewise, Bouriaud et al. (2019) recently highlighted that local calibration of stem taper equations resulted in small gains and high biases but found two Bayesian approaches to perform significantly better. As discussed further in section 5, terrestrial laser scanning (TLS) now offers the unprecedented opportunity to generate necessary stem taper equation calibration data with millimetre levels of accuracy. Saarinen et al. (2019) suggested that at least 50 trees with TLS were needed to effectively calibrate an existing stem taper equation, but they demonstrated improvements in the lower portion of the bole with only one sample tree due to the large number of observations generated by TLS. Clearly, local calibration with or even without new observations is an important and effective method to ensure the proper application of stem taper equations.

4.3. Evaluation

Given the wide application and use of stem taper equations for estimating both total and merchantable volume, effective evaluation of these equations is important yet often overlooked in practice. As previously described, calibration of stem taper equations can be achieved with relatively few observations but often requires the availability of independent data, which can be hard to obtain because of the difficulties and expense of measuring upper-stem diameters. Consequently, evaluation of stem taper equations can be done using either stem diameters or stem volumes or a combination of both, which is generally preferred and often most revealing (Li and Weiskittel 2010; Shahzad et al. 2020).

Kozak and Smith (1993) offered several practical quantitative approaches for evaluating stem taper equations, which rely on rankings of absolute values. In contrast, Goodwin (2009) suggested the use of mean scaled statistics for more effective comparisons. If only stem diameters are available, examining behavior across relative height classes is important, particularly equation performance on the lower half of the bole. Likewise, examining performance across tree DBH classes is critical if only stem volume is available. Cross-validation or even bootstrapping methods for evaluation can be informative but might be unnecessary, especially when data are limited (Kozak and Kozak 2003). Equivalence testing can be useful, as a region of indifference can be selected by the user to handle potential measurement differences in the available data or to better define practically meaningful differences (e.g., Zakrzewski and MacFarlane 2006). In contrast to purely quantitative assessments, both Goodwin (2009) and Zakrzewski (2009) provided various qualitative benchmarks for stem taper equations (Table 5). Using either quantitative or qualitative measures, the proper and routine evaluation of stem taper equations is required because of the myriad of factors that can influence their overall performance.

4.4. Application and use

Because of their high flexibility, taper equations have a variety of uses, including (*i*) describing absolute or relative changes in tree form, (*ii*) computing upper-stem diameters at specific locations on the bole, (*iii*) deriving volume estimates for portions or the entire stem, and (*iv*) merchandizing trees into specific products based on certain specifications like log length or small- or large-end diameter, which are all much harder to achieve with a volume equation. Important considerations for a taper equation's most effective application and use are (*i*) interval bolt length and method for numerical integration when required,

Table 5. Qualitative criteria for evaluating and assessing stem taper equations applied to common forms.

	Model form					
Criterion	Bi (2000)	Goodwin (2009)	Max and Burkhart (1976)	Kozak (2004)	Random forest	Zakrzewski (1999)
Closed-form integral expression and invertible	0	1	1	0	0	1
Allows flexibility of diameter input	0	1	0	0	0	0
Applicable to a wide range of tree sizes and species	1	1	1	1	1	1
Constrained[a]	0	0	0	0	0	1
Nonsegmented	1	1	0	1	1	1
Defines a stem surface in a closed form	0	0	0	0	0	0
Easily localized[b]	0	1	0.5	0	0	1
Easily regionalizable[c]	1	1	1	1	0	1
Has full continuity from stem base to tip[d]	0.5	1	0	1	1	1
Uses easy-to-obtain variables	1	1	1	1	1	1
Total	4.5	8	4.5	5	4	8

Note: 1 = yes; 0 = no. Table was adapted from Goodwin (2009) and Zakrzewski (2009).

[a]Predictions should be consistent with inputs and yield logical values (e.g., d_u = DBH when h_u = 1.3 m).

[b]Able to explain between-tree variability with inclusion of additional information such as upper-stem diameters.

[c]Applicable across broad spatial scales and reflects regional differences due to environmental or management-related factors without the need for reparameterization.

[d]Provides logical predictions throughout the full range of 0 to H for all trees.

(*ii*) deriving estimates of inside- and outside-bark diameter, and (*iii*) measurement or imputation of stem taper equation covariates.

Most of the highly flexible variable-form taper equations (e.g., Kozak 2004) require numerical integration, which can be computationally demanding especially for large forest inventories. With this approach, stem diameters are predicted by the taper equation and volumes derived with the use of cubic log volume formulas such as Smalian, Huber, and Newton. Likewise, various log rules exist when volume in board feet is needed. In addition to the method of integration, an important additional consideration is the actual interval length for numerical integration, with 1–2 m as the most common recommendation for computation of cubic volume, but errors can rapidly increase above those intervals (Goulding 1979; Biging 1988). As highlighted by Filho and Schaaf (1999), numerical integration methods done at even 2 m will generally underestimate true volume, and they recommend Huber's method, as it is more robust. When computing board-foot volume, the log length will depend upon the specific log rule, but rarely is the length < 5 m. Briggs (1994) used several illustrations to demonstrate how shorter logs create more board-foot volume. Hence, log buyers often stipulate a minimum mean log length in contracts to prevent excessive "volume manufacturing".

For practical reasons, inside-bark diameter or volume is often preferred given the limited value of bark. However, predictions of both inside and outside bark are often needed at times. Stem taper equations can be developed for both inside and outside bark, but inside-bark observations might be more limited if standing tree taper data sets are included (e.g., Clark et al. 1991; Li et al. 2012). In addition, Li and Weiskittel (2011) found that inside-bark diameters were better predicted using bark thickness equations that included diameter outside bark as a predictor when compared with the sole use of a stem taper equation. Consequently, a potentially more robust system for estimating both inside- and outside-bark diameter might be using a stem taper equation to predict the latter and a bark thickness equation for the former (Li and Weiskittel 2011).

As previously described, most stem taper equations rely primarily on DBH and total height as covariates, but additional variables like crown ratio or upper-stem diameters might also be needed. As previously mentioned, measurement or predicted error associated with covariates, especially upper-stem diameter (Westfall et al. 2016), can be problematic and result in significant biases. Equations such as eq. 54 can be used to estimate an upper-stem diameter at a knot transition between segments, but they can introduce another source of uncertainty. For example, Clark et al. (1991) developed an equation to predict upper-stem diameter equations for a variety of species in the southern US, but it required both tree DBH and total height and had a coefficient of variation ranging from 2% to 11%. Because stem taper equations require DBH, alternative methods are often needed to determine the form and volume of either saplings or seedlings in a forest inventory. The stem taper equation of Goodwin (2009) uses diameter at a flexible yet known height and is one of the few that does not rely on DBH, which would ensure applicability to either seedlings or saplings.

Most importantly, only a subsample (5%–30%) of tree heights are generally measured in a typical forest inventory, and the remaining values must be imputed using regional or locally calibrated equations. Garber et al. (2009) evaluated the effects of various height imputation approaches on stand volume estimates and found that the root mean square error (RMSE) ranged from 10 to 65 $m^3 \cdot ha^{-1}$ or 3% to 21% depending on the method and number of trees available for local calibration. Their recommendation was the use of a regional equation that included factors in addition to tree DBH such as stand density or locally calibrating a mixed-effects model with at least four randomly selected trees within a stand. The same findings would likely hold for other factors like crown ratio, whereas unbiased estimates of stand density would also be needed if stand-level factors are used as a model covariate. This is important, as uncertainty in tree-level volume estimates caused by measurement or prediction error can significantly compound when being summarized to larger scales (e.g., Berger et al. 2014; McRoberts and Westfall 2016).

5. Synthesis and future

Clearly, stem taper equations have a long history of development, application, and use. Model forms, parameterization, and issues with their application have continued to be refined over the past several decades as outlined in this review. General consensus appears to be converging on (*i*) clear advantages of the variable-form model type; (*ii*) the importance of including additional factors beyond tree DBH and height, except potentially upper-stem diameters; (*iii*) the superiority of a regionally calibrated method or semi- and nonparametric methods when refined and localized estimates are needed, assuming sufficient

data are available; and (*iv*) the importance of the specific method and length of the numerical integration interval, as well as the availability of quality input data when applying taper equations to forest inventory data, particularly at large spatial scales.

Going forward, a variety of new and emerging technologies will continue to improve taper equations and their predictive capacity. Currently, the most important is TLS, which provides an unprecedented level of detail on stem form and quantity and quality of data for modeling. Numerous studies on this topic covering a variety of algorithms, sensors, and applications are now available; the studies highlighted here represent only a small number of them. For example, Saarinen et al. (2017) demonstrated the feasibility of using TLS to accurately measure stem taper and volume across multiple hardwood and softwood species with scans taking between 20 and 30 min or one-sixth the amount of time required to do traditional destructive sampling. This potential time and cost savings while providing a high resolution of data should allow for the greater sample sizes needed for better capturing the within- and between-tree variation in stem form, which is important for species with eccentric forms (Puletti et al. 2019). This also potentially allows the assessment of stem volume growth over time (Luoma et al. 2019), which in turn makes possible the ability to develop more dynamic stem taper equations. Clearly, TLS can result in better stem form data that help lead to better calibrated (Saarinen et al. 2019) or more refined (Sun et al. 2016) taper equations.

Even so, TLS can only measure outside-bark diameters, can be costly, requires significant processing, struggles to separate the bole from branches in the tree crown, and can be complicated in areas with complex terrain or rich understories (Heinzel and Huber 2016). Recently, Eliopoulos et al. (2020) showed that terrestrial stereoscopic photogrammetry was able to measure tree diameters faster and cheaper than typical TLS scanners. Another important yet potentially underutilized source of taper data in North America is from the digital files created by mechanized harvesters, which have been used more effectively for this purpose in Australia and New Zealand (e.g., Murphy et al. 2006) and Scandinavia (e.g., Koskela et al. 2006). For better characterizing inside-bark stem form, additional technologies are also available. On logs or other destructively sampled trees, computed tomography (CT) can be used to accurately characterize bark thickness and its variation (e.g., Stängle et al. 2016). On standing trees, ultrasonic and thermal image technologies have been used to nondestructively detect internal defects (Taskhiri et al. 2020). These methods combined with TLS may offer a novel means for modeling wood quality and net volume or at least allow for better ways of quantifying defects than achieved in prior analyses (Frank et al. 2018).

Overall, stem volume remains one of the most important tree- and stand-level attributes for forest inventories, management, and planning. This review has highlighted the extent and breadth of scientific literature on stem taper equations, which have become the primary means for estimating stem volume. Despite the great progress made in accurately predicting stem taper and the availability of new technologies for better measuring it, many important challenges remain. Future efforts should address (*i*) developing more biologically based models of stem form and growth (Mäkelä and Valentine 2020); (*ii*) constructing geographically representative, species-specific, and nationally consistent stem taper and volume databases (e.g., Radtke et al. 2015; Frank et al. 2019); (*iii*) better quantifying the uncertainty of tree DBH, height, or volume and its potential to compound across spatial scales (e.g., McRoberts and Westfall 2016); (*iv*) the application of consistent, robust, and tractable methodologies for national inventories (e.g., Weiskittel et al. 2020); and (*v*) the full integration of multiple available technologies for improving estimation procedures. These and many other challenges will likely be the key focal areas for future research in the years to come.

Acknowledgements

The authors appreciate the suggestion and encouragement of Phil Burton to draft this review. Helpful feedback from Meg Fergusson, Associate Editor Thomas Nord-Larsen, and two reviewers significantly improved a previous version of this manuscript. Funding was provided by the US Forest Service, Forest Inventory and Analysis Program's National Scale Biomass Estimators project and the National Science Foundation's Center for Advanced Forestry Systems (Award No. 1915078).

References

Anuchin, N.P. 1960. Forest mensuration. 2nd ed. Goslebumizdat, Moscow, Leningrad. 454pp.

Avery, T.E., and Burkhart, H.E. 2002. Forest measurements. 5th ed. Waveland Press, Inc., Long Grove, Ill. 480pp.

Behre, C.E. 1927. Form-class taper curves and volume tables and their application. J. Agric. Res. **35**: 673–744.

Behre, E., Bruce, D., Munns, E., Chapman, H., Hansen, T., Mason, D., et al. 1926. Methods of preparing volume and yield tables: Report of the committee on standardization of volume and yield tables. J. For. **24**: 653–666. doi:10.1093/jof/24.6.653.

Berger, A., Gschwantner, T., McRoberts, R.E., and Schadauer, K. 2014. Effects of measurement errors on individual tree stem volume estimates for the Austrian National Forest Inventory. For. Sci. **60**(1): 14–24. doi:10.5849/forsci.12-164.

Bi, H. 2000. Trigonometric variable-form taper equations for Australian eucalypts. For. Sci. **46**: 397–409. doi:10.1093/forestscience/46.3.397.

Biging, G.S. 1988. Estimating the accuracy of volume equations using taper equations of stem profile. Can. J. For. Res. **18**(8): 1002–1007. doi:10.1139/x88-153.

Bitterlich, W. 1984. The relascope idea: relative measurements in forestry. Commonwealth Agricultural Bureaux, Wallingford, U.K. 242pp.

Bouriaud, O., Stefan, G., and Saint-André, L. 2019. Comparing local calibration using random effects estimation and Bayesian calibrations: a case study with a mixed effect stem profile model. Ann. For. Sci. **76**: 65. doi:10.1007/s13595-019-0848-5.

Briggs, D.G. 1994. Forest products measurements and conversion factors: with special emphasis on the U.S. Pacific Northwest. Contribution No. 75. University of Washington. Institute of Forest Resources, Seattle, Wash.

Brink, C., and von Gadow, K. 1983. Modelling stem profiles. South Afr. For. J. **127**(1): 23–25. doi:10.1080/00382167.1983.9628909.

Bruce, D. 1972. Some transformations of the Behre equation of tree form. For. Sci. **18**: 164–166. doi:10.1093/forestscience/18.2.164.

Bruce, D. 1982. Butt log volume estimators. For. Sci. **28**: 489–503. doi:10.1093/forestscience/28.3.489.

Bruce, D., and Schumacher, F.X. 1942. Forest mensuration. McGraw-Hill Book Company, Inc., New York. 425pp.

Bullock, B.P., and Burkhart, H.E. 2003. Equations for predicting green weight of loblolly pine trees in the South. South. J. Appl. For. **27**(3): 153–159. doi:10.1093/sjaf/27.3.153.

Burkhart, H.E. 1977. Cubic-foot volume of loblolly pine to any merchantable top limit. South. J. Appl. For. **1**(2): 7–9. doi:10.1093/sjaf/1.2.7.

Burkhart, H.E., and Tomé, M. 2012. Modeling forest trees and stands. Springer Science & Business Media, Berlin, Germany. 458pp.

Burkhart, H.E., and Walton, S.B. 1985. Incorporating crown ratio into taper equations for loblolly pine trees. For. Sci. **31**: 478–484.

Cao, Q.V. 2009. Calibrating a segmented taper equation with two diameter measurements. South. J. Appl. For. **33**(2): 58–61. doi:10.1093/sjaf/33.2.58.

Cao, Q.V., and Burkhart, H.E. 1980. Cubic-foot volume of loblolly pine to any height limit. South. J. Appl. For. **4**(4): 166–168. doi:10.1093/sjaf/4.4.166.

Cao, Q.V., and Wang, J. 2011. Calibrating fixed- and mixed-effects taper equations. For. Ecol. Manage. **262**(4): 671–673. doi:10.1016/j.foreco.2011.04.039.

Cao, Q.V., and Wang, J. 2015. Evaluation of methods for calibrating a tree taper equation. For. Sci. **61**(2): 213–219. doi:10.5849/forsci.14-008.

Castle, M., Weiskittel, A., Wagner, R., Ducey, M., Frank, J., and Pelletier, G. 2017. Variation in stem form and risk of four commercially important hardwood species in the Acadian Forest: implications for potential sawlog volume and tree classification systems. Can. J. For. Res. **47**(11): 1457–1467. doi:10.1139/cjfr-2017-0182.

Castle, M., Weiskittel, A., Wagner, R., Ducey, M., Frank, J., and Pelletier, G. 2018. Evaluating the influence of stem form and damage on individual-tree diameter increment and survival in the Acadian Region: implications for predicting future value of northern commercial hardwood stands. Can. J. For. Res. **48**(9): 1007–1019. doi:10.1139/cjfr-2018-0081.

Catmull, E., and Rom, R., 1974. A class of local interpolating splines. *In* Computer aided geometric design. *Edited by* R.E. Barnhill and R.F. Riesenfeld. Academic Press. pp. 317–326. doi:10.1016/B978-0-12-079050-0.50020-5.

Clark, A.C., III, Souter, R.A., and Schlaegel, B.E. 1991. Stem profile equations for southern tree species. Res. Pap. SE-282, U.S. Department of Agriculture,

Forest Service, Southeastern Forest Experiment Station, Asheville, N.C. 117pp.
Clutter, J.L. 1980. Development of taper functions from variable-top merchantable volume equations. For. Sci. **26**: 117–120. doi:10.1093/forestscience/26.1.117.
Cormier, K.L., Reich, R.M., Czaplewski, R.L., and Bechtold, W.A. 1992. Evaluation of weighted regression and sample size in developing a taper model for loblolly pine. For. Ecol. Manage. **53**(1-4): 65–76. doi:10.1016/0378-1127(92)90034-7.
Dean, T.J., Roberts, S.D., Gilmore, D.W., Maguire, D.A., Long, J.N., O'Hara, K.L., and Seymour, R.S. 2002. An evaluation of the uniform stress hypothesis based on stem geometry in selected North American conifers. Trees, **16**(8): 559–568. doi:10.1007/s00468-002-0208-0.
Demaerschalk, J.P. 1972. Converting volume equations to compatible taper equations. For. Sci. **18**(3): 241–245. doi:10.1093/forestscience/18.3.241.
de-Miguel, S., Mehtätalo, L., Shater, Z., Kraid, B., and Pukkala, T. 2012. Evaluating marginal and conditional predictions of taper models in the absence of calibration data. Can. J. For. Res. **42**(7): 1383–1394. doi:10.1139/x2012-090.
Duan, A., Zhang, S., Zhang, X., and Zhang, J. 2016. Development of a stem taper equation and modelling the effect of stand density on taper for Chinese fir plantations in southern China. PeerJ. **4**: e1929. doi:10.7717/peerj.1929. PMID:27168964.
Eliopoulos, N.J., Shen, Y., Nguyen, M.L., Arora, V., Zhang, Y., Shao, G., et al. 2020. Rapid tree diameter computation with terrestrial stereoscopic photogrammetry. J. For. **118**(4): 355–361. doi:10.1093/jofore/fvaa009.
Fang, Z., Borders, B.E., and Bailey, R.L. 2000. Compatible volume-taper models for loblolly and slash pine based on a system with segmented-stem form factors. For. Sci. **46**: 1–12. doi:10.1093/forestscience/46.1.1.
Filho, A.F., and Schaaf, L.B. 1999. Comparison between predicted volumes estimated by taper equations and true volumes obtained by the water displacement technique (xylometer). Can. J. For. Res. **29**(4): 451–461. doi:10.1139/x99-013.
Flewelling, J.W., and Raynes, L.M. 1993. Variable-shape stem-profile predictions for western hemlock. Part I. Predictions from DBH and total height. Can. J. For. Res. **23**(3): 520–536. doi:10.1139/x93-070.
Fogelberg, S.E. 1953. Volume charts based on absolute form class. Louisiana Tech Forestry Club of Louisiana Polytechnic Institute, Ruston, La.
Frank, J., Castle, M.E., Westfall, J.A., Weiskittel, A.R., MacFarlane, D.W., Baral, S.K., et al. 2018. Variation in occurrence and extent of internal stem decay in standing trees across the eastern US and Canada: evaluation of alternative modelling approaches and influential factors. Forestry, **91**(3): 382–399. doi:10.1093/forestry/cpx054.
Frank, J., Weiskittel, A., Walker, D., Westfall, J.A., Radtke, P.J., Affleck, D.L., Coulston, J., and MacFarlane, D.W. 2019. Gaps in available data for modeling tree biomass in the United States. Gen. Tech. Rep. NRS-184, U.S. Department of Agriculture, Forest Service, Northern Research Station, Newtown Square, Pa. 57pp.
Gallant, A.R., and Fuller, W.A. 1973. Fitting segmented polynomial regression models whose join points have to be estimated. J. Am. Stat. Assoc. **68**(341): 144–147. doi:10.1080/01621459.1973.10481353.
Garber, S.M., and Maguire, D.A. 2003. Modeling stem taper of three central Oregon species using nonlinear mixed effects models and autoregressive error structures. For. Ecol. Manage. **179**(1–3): 507–522. doi:10.1016/S0378-1127(02)00528-5.
Garber, S.M., Temesgen, H., Monleon, V.J., and Hann, D.W. 2009. Effects of height imputation strategies on stand volume estimation. Can. J. For. Res. **39**(3): 681–690. doi:10.1139/X08-188.
Gómez-García, E., Crecente-Campo, F., and Diéguez-Aranda, U. 2013. Selection of mixed-effects parameters in a variable–exponent taper equation for birch trees in northwestern Spain. Ann. For. Sci. **70**(7): 707–715. doi:10.1007/s13595-013-0313-9.
Goodwin, A.N. 2009. A cubic tree taper model. Aust. For. **72**(2): 87–98. doi:10.1080/00049158.2009.10676294.
Goulding, C.J. 1979. Cubic spline curves and calculation of volume of sectionally measured trees. N.Z. J. For. Sci. **9**: 89–99.
Goulding, C.J., and Murray, J.C. 1976. Polynomial taper equations that are compatible with tree volume equations. N.Z. J. For. Sci. **5**: 313–322.
Gray, H.R. 1956. The form and taper of forest-tree stems. Institute Paper 32, Imperial Forestry Institute, University of Oxford, Oxford, U.K.
Gregoire, T.G., and Schabenberger, O. 1996. A non-linear mixed-effects model to predict cumulative bole volume of standing trees. J. Appl. Stat. **23**(2–3): 257–272. doi:10.1080/02664769624233.
Grosenbaugh, L.R. 1966. Tree form: definition, interpolation, extrapolation. For. Chron. **42**(4): 444–457. doi:10.5558/tfc42444-4.
Hann, D.W. 1994. A key to the literature presenting tree volume and taper equations for species in the Pacific Northwest and California. Research Contribution 6, Oregon State University, Forest Research Laboratory, Corvallis, Ore.
Hann, D.W., Walters, D.K., and Scrivani, J.A. 1987. Incorporating crown ratio into prediction equations for Douglas fir stem volume. Can. J. For. Res. **17**(1): 17–22. doi:10.1139/x87-003.
Harrell, F.E., Jr. 2015 Regression modeling strategies: With applications to linear models, logistic and ordinal regression, and survival analysis. Springer, Berlin, Germany. 582pp.
Heinzel, J., and Huber, M.O. 2016. Detecting tree stems from volumetric TLS data in forest environments with rich understory. Remote Sens. **9**(1): 9. doi:10.3390/rs9010009.
Hohenadl, W. 1924. Der Aufbau der Baumschäfte. Forstwiss. Centralbl. **46**: 460–470, 495–508.
Hojer, A.G. 1903. Tallens och granens tillvaxt. Biharg till Fr. Lovén. Om vara barrskogar. Stockholm, Norway.
Hradetzky, J. 1976. Analyse und interpretation statistisher abränger keiten. Mitteilungen der Forstlichen Versuchs-und Forschng sanstalt Baden-Wüettemberg. Heft Nr: 146.
Huang, S., Price, D., Morgan, D., and Peck, K. 2000. Kozak's variable-exponent taper equation regionalized for white spruce in Alberta. West. J. Appl. For. **15**(2): 75–85. doi:10.1093/wjaf/15.2.75.
Jordan, L., Berenhaut, K., Souter, R., and Daniels, R.F. 2005. Parsimonious and completely compatible taper, total, and merchantable volume models. For. Sci. **51**: 578–584.
Kershaw, J.A., Jr., Ducey, M.J., Beers, T.W., and Husch, B. 2016. Forest mensuration. 5th ed. John Wiley & Sons, Oxford, U.K. 630pp.
Kilkki, P., Saramäki, M., and Varmola, M. 1978. A simultaneous equation model to determine taper curve. Silva Fenn. **12**(2): 4995. doi:10.14214/sf.a14849.
Kitikidou, K., and Chatzilazarou, G. 2008. Estimating the sample size for fitting taper equations. J. For. Sci. **54**(No. 4): 176–182. doi:10.17221/789-JFS.
Koskela, L., Nummi, T., Wenzel, S., and Kivinen, V.-P. 2006. On the analysis of cubic smoothing spline-based stem curve prediction for forest harvesters. Can. J. For. Res. **36**(11): 2909–2919. doi:10.1139/x06-165.
Kozak, A. 1988. A variable-exponent taper equation. Can. J. For. Res. **18**(11): 1363–1368. doi:10.1139/x88-213.
Kozak, A. 1997. Effects of multicollinearity and autocorrelation on the variable-exponent taper functions. Can. J. For. Res. **27**(5): 619–629. doi:10.1139/x97-011.
Kozak, A. 1998. Effects of upper stem measurements on the predictive ability of a variable-exponent taper equation. Can. J. For. Res. **28**(7): 1078–1083. doi:10.1139/x98-120.
Kozak, A. 2004. My last words on taper equations. For. Chron. **80**(4): 507–515. doi:10.5558/tfc80507-4.
Kozak, A., and Kozak, R. 2003. Does cross validation provide additional information in the evaluation of regression models? Can. J. For. Res. **33**(6): 976–987. doi:10.1139/x03-022.
Kozak, A., and Smith, J.H.G. 1993. Standards for evaluating taper estimating systems. For. Chron. **69**(4): 438–444. doi:10.5558/tfc69438-4.
Kozak, A., Munro, D.D., and Smith, J.H.G. 1969. Taper functions and their application in forest inventory. For. Chron. **45**(4): 278–283. doi:10.5558/tfc45278-4.
Kozitsin, P.D. 1909. Teoreticheskaya proverka udel'nykh massovykh tablits dlya breezy. 111, Trudy Moskovskogo Lesnogo Obshchestva.
Kublin, E., and Breidenbach, J. 2013. TapeR version 0.3.2. R Package. R Foundation for Statistical Computing, Vienna, Austria.
Kublin, E., Augustin, N.H., and Lappi, J. 2008. A flexible regression model for diameter prediction. Eur. J. For. Res. **127**(5): 415–428. doi:10.1007/s10342-008-0225-7.
Kublin, E., Breidenbach, J., and Kändler, G. 2013. A flexible stem taper and volume prediction method based on mixed-effects B-spline regression. Eur. J. For. Res. **132**(5–6): 983–997. doi:10.1007/s10342-013-0715-0.
Kuželka, K., and Marušák, R. 2014*a*. Use of nonparametric regression methods for developing a local stem form model. J. For. Sci. **60**: 464–471. doi:10.17221/56/2014-JFS.
Kuželka, K., and Marušák, R. 2014*b*. Comparison of selected splines for stem form modeling: A case study in Norway spruce. Ann. For. Res. **57**: 137–148. doi:10.15287/afr.2014.177.
Laasasenaho, J., Melkas, T., and Aldén, S. 2005. Modelling bark thickness of *Picea abies* with taper curves. For. Ecol. Manage. **206**(1–3): 35–47. doi:10.1016/j.foreco.2004.10.058.
Lappi, J. 2006. A multivariate, nonparametric stem-curve prediction method. Can. J. For. Res. **36**(4): 1017–1027. doi:10.1139/x05-305.
Larson, P.R. 1963. Stem form development of forest trees. For. Sci. Monogr. **9** (suppl_2): a0001–42. doi:10.1093/forestscience/9.s2.a0001.
Leites, L.P., and Robinson, A.P. 2004. Improving taper equations of loblolly pine with crown dimensions in a mixed-effects modeling framework. For. Sci. **50**: 204–212. doi:10.1093/forestscience/50.2.204.
Li, R., and Weiskittel, A.R. 2010. Comparison of model forms for estimating stem taper and volume in the primary conifer species of the North American Acadian Region. Ann. For. Sci. **67**(3): 302–302. doi:10.1051/forest/2009109.
Li, R., and Weiskittel, A.R. 2011. Estimating and predicting bark thickness for seven conifer species in the Acadian Region of North America using a mixed-effects modeling approach: comparison of model forms and subsampling strategies. Eur. J. For. Res. **130**(2): 219–233. doi:10.1007/s10342-010-0423-y.
Li, R., Weiskittel, A., Dick, A.R., Kershaw, J.A., and Seymour, R.S. 2012. Regional stem taper equations for eleven conifer species: development and assessment. North. J. Appl. For. **29**(1): 5–14. doi:10.5849/njaf.10-037.
Liu, Y., Trancoso, R., Ma, Q., Yue, C., Wei, X., and Blanco, J.A. 2020*a*. Incorporating climate effects in Larix gmelinii improves stem taper models in

the Greater Khingan Mountains of Inner Mongolia, northeast China. For. Ecol. Manage. **464**: 118065. doi:10.1016/j.foreco.2020.118065.

Liu, Y., Yue, C., Wei, X., Blanco, J.A., and Trancoso, R. 2020*b*. Tree profile equations are significantly improved when adding tree age and stocking degree: an example for *Larix gmelinii* in the Greater Khingan Mountains of Inner Mongolia, northeast China. Eur. J. For. Res. **139**(3): 443–458. doi:10.1007/s10342-020-01261-z.

López-Martínez, J.O., Vargas-Larreta, B., Aguirre-Calderón, O.A., Aguirre-Calderón, C.G., Macario-Mendoza, P.A., Martínez-Salvador, M., and Álvarez-González, J.G. 2020. Compatible taper-volume systems for major tropical species in Mexico. Forestry, **93**: 56–74. doi:10.1093/forestry/cpz033.

Luoma, V., Saarinen, N., Kankare, V., Tanhuanpää, T., Kaartinen, H., Kukko, A., et al. 2019. Examining changes in stem taper and volume growth with two-date 3D point clouds. Forests, **10**(5): 382. doi:10.3390/f10050382.

Lynch, T.B., Zhao, D., Harges, W., and McTague, J.P. 2017. Deriving compatible taper functions from volume ratio equations based on upper-stem height. Can. J. For. Res. **47**(10): 1424–1431. doi:10.1139/cjfr-2017-0108.

MacFarlane, D.W. 2010. Predicting branch to bole volume scaling relationships from varying centroids of tree bole volume. Can. J. For. Res. **40**(12): 2278–2289. doi:10.1139/X10-168.

MacFarlane, D.W., and Weiskittel, A.R. 2016. A new method for capturing stem taper variation for trees of diverse morphological types. Can. J. For. Res. **46**(6): 804–815. doi:10.1139/cjfr-2016-0018.

Madsen, S.F. 1985. Compatible tree taper and volume functions for five different conifers. Forstl. Forsoegsvaes. **40**: 95–140.

Mäkelä, A., and Valentine, H.T. 2020. Models of tree and stand dynamics: theory, formulation and application. Springer International Publishing, Berlin, Germany. 310pp.

Marchi, M., Scotti, R., Rinaldini, G., and Cantiani, P. 2020. Taper function for *Pinus nigra* in central Italy: Is a more complex computational system required? Forests, **11**(4): 405. doi:10.3390/f11040405.

Martin, J.A. 1981. Taper and volume equations for selected Appalachian hardwood species. Res. Pap. NE-490. U.S. Department of Agriculture, Forest Service. 22pp.

Matney, T.G., Hodges, J.D., Sullivan, A.D., and Ledbetter, J.R. 1985. Tree profile and volume ratio equations for sweetgum and cherrybark oak trees. South. J. Appl. For. **9**(4): 222–227. doi:10.1093/sjaf/9.4.222.

Max, T.A., and Burkhart, H.E. 1976. Segmented polynomial regression applied to taper equations. For. Sci. **22**: 283–289. doi:10.1093/forestscience/22.3.283.

McRoberts, R.E., and Westfall, J.A. 2016. Propagating uncertainty through individual tree volume model predictions to large-area volume estimates. Ann. For. Sci. **73**(3): 625–633. doi:10.1007/s13595-015-0473-x.

McTague, J.P., and Bailey, R.L. 1987. Compatible basal area and diameter distribution models for thinned loblolly pine plantations in Santa Catarina. Braz. For. Sci. **33**: 43–51. doi:10.1093/forestscience/33.1.43.

Mesavage, C. 1947. Tables for estimating cubic-foot volume of timber. Pap. US Forest Serv. Southern Forest Exp. Sta, New Orleans, La. 111.

Mesavage, C., and Girard, J.W. 1946. Tables for estimating board-foot volume of timber. US Forest Service, Southern Forest Experiment Station, New Orleans, La. 94 pp.

Metzger, K. 1893. Der Wind als maßgebender Faktor für das Wachsthum der Bäume. Mündener Forstliche Hefte. **5**: 35–86.

Muhairwe, C.K., LeMay, V.M., and Kozak, A. 1994. Effects of adding tree, stand, and site variables to Kozak's variable-exponent taper equation. Can. J. For. Res. **24**(2): 252–259. doi:10.1139/x94-037.

Murphy, G., Wilson, I., and Barr, B. 2006. Developing methods for pre-harvest inventories which use a harvester as the sampling tool. Aust. For. **69**(1): 9–15. doi:10.1080/00049158.2006.10674982.

Narmontas, M., Rupšys, P., and Petrauskas, E. 2020. Models for tree taper form: The Gompertz and Vasicek diffusion processes framework. Symmetry, **12**(1): 80. doi:10.3390/sym12010080.

Newnham, R.M. 1988. A variable-form taper function. Information Report PI-X-083, Petawawa National Forestry Institute, Chalk River, Ont.

Newnham, R.M. 1992. Variable-form taper functions for four Alberta tree species. Can. J. For. Res. **22**(2): 210–223. doi:10.1139/x92-028.

Nicoletti, M.F., Carvalho, S.deP.C.E., Machado, S.doA., Costa, V.J., Silva, C.A., and Topanotti, L.R. 2020. Bivariate and generalized models for taper stem representation and assortments production of loblolly pine (*Pinus taeda* L.). J. Environ. Manage. **270**: 110865. doi:10.1016/j.jenvman.2020.110865. PMID:32721311.

Nigh, G., and Smith, W. 2012. Effect of climate on lodgepole pine stem taper in British Columbia. Can. For. **85**(5): 579–587. doi:10.1093/forestry/cps063.

Nunes, M.H., and Görgens, E.B. 2016. Artificial intelligence procedures for tree taper estimation within a complex vegetation mosaic in Brazil. PLoS ONE, **11**(5): e0154738. doi:10.1371/journal.pone.0154738. PMID:27187074.

Ormerod, D.W. 1973. A simple bole model. For. Chron. **49**(3): 136–138. doi:10.5558/tfc49136-3.

ÖzçeliĶ, R., and Bal, C. 2013. Effects of adding crown variables in stem taper and volume predictions for black pine. Turk. J. Agric. For. **37**: 231–242.

Özçelik, R., and Cao, Q.V. 2017. Evaluation of fitting and adjustment methods for taper and volume prediction of black pine in Turkey. For. Sci. **63**(4): 349–355. doi:10.5849/FS.2016-067.

Ozçelik, R., Diamantopoulou, M.J., Brooks, J.R., and Wiant, H.V., Jr. 2010. Estimating tree bole volume using artificial neural network models for four species in Turkey. J. Environ. Manage. **91**(3): 742–753. doi:10.1016/j.jenvman.2009.10.002. PMID:19880241.

Özçelik, R., Karatepe, Y., Gürlevik, N., Cañellas, I., and Crecente-Campo, F. 2016. Development of ecoregion-based merchantable volume systems for *Pinus brutia* Ten. and *Pinus nigra* Arnold. in southern Turkey. J. For. Res. **27**(1): 101–117. doi:10.1007/s11676-015-0147-4.

Özçelik, R., Diamantopoulou, M.J., and Trincado, G. 2019. Evaluation of potential modeling approaches for Scots pine stem diameter prediction in north-eastern Turkey. Comput. Electron. Agric. **162**: 773–782. doi:10.1016/j.compag.2019.05.033.

Pang, L., Ma, Y., Sharma, R.P., Rice, S., Song, X., and Fu, L. 2016. Developing an improved parameter estimation method for the segmented taper equation through combination of constrained two-dimensional optimum seeking and least square regression. Forests, **7**(12): 194. doi:10.3390/f7090194.

Pedan, A. 2003. Smoothing with SAS Proc Mixed. Seattle SAS Users Group International Proceedings, Seattle, Wash.

Pelletier, G., Landry, D., Girouard, M., and Brunswick, I.N. 2014. A tree classification system for New Brunswick. Northern Hardwoods Research Institute, Edmundston, New Brunswick.

Penfound, W.T. 1934. Comparative structure of the wood in the "knees," swollen bases, and normal trunks of the tupelo gum (*Nyssa aquatica* L.). Am. J. Bot. **21**(10): 623–631. doi:10.1002/j.1537-2197.1934.tb04991.x.

Poudel, K.P., Özçelik, R., and Yavuz, H. 2020. Differences in stem taper of black alder (*Alnus glutinosa* subsp. *barbata*) by origin. Can. J. For. Res. **50**(6): 581–588. doi:10.1139/cjfr-2019-0314.

Pressler, M.R. 1864. Das gesetz der stammbildung. Arnoldische Buchhandlung, Leipzig, Germany.

Puletti, N., Grotti, M., and Scotti, R. 2019. Evaluating the eccentricities of poplar stem profiles with terrestrial laser scanning. Forests, **10**(3): 239. doi:10.3390/f10030239.

Quiñonez-Barraza, G., Zhao, D., and De los Santos-Posadas, H.M. 2019. Compatible taper and stem volume equations for five pine species in mixed-species forests in Mexico. For. Sci. **65**(5): 602–613. doi:10.1093/forsci/fxz030.

Radtke, P.J., Walker, D.M., Weiskittel, A.R., Frank, J., Coulston, J.W., and Westfall, J.A., 2015. Legacy tree data: a national database of detailed tree measurements for volume, weight, and physical properties. *In* Pushing boundaries: new directions in inventory techniques and applications: Forest Inventory and Analysis (FIA) symposium 2015, 8–10 December 2015, Portland, Ore. USDA For. Serv. Gen. Tech. Rep. PNW-GTR-931. *Compiled by* S.M. Stanton and G.A. Christensen. US Department of Agriculture, Forest Service, Pacific Northwest Research Station, Portland, Ore. pp. 25–30.

Reed, D.D., and Green, E.J. 1984. Compatible stem taper and volume ratio equations. For. Sci. **30**: 977–990.

Riemer, T., von Gadow, K., and Sloboda, B. 1995. Ein Modell zur Beschreibung von Baumschäften. Allgemeine Forst-und Jagdzeitung, **166**: 144–147.

Robinson, A.P., and Hamann, J.D. 2011. Forest analytics with R: an introduction. Springer, New York.

Robinson, A.P., Lane, S.E., and Thérien, G. 2011. Fitting forestry models using generalized additive models: a taper model example. Can. J. For. Res. **41**(10): 1909–1916. doi:10.1139/x11-095.

Rojo, A., Perales, X., Sanchez-Rodriguez, F., Alvarez-Gonzalez, J.G., and von Gadow, K. 2005. Stem taper functions for maritime pine (*Pinus pinaster* Ait.) in Galicia (Northwestern Spain). Eur. J. For. Res. **124**(3): 177–186. doi:10.1007/s10342-005-0066-6.

Saarinen, N., Kankare, V., Vastaranta, M., Luoma, V., Pyörälä, J., Tanhuanpää, T., et al. 2017. Feasibility of terrestrial laser scanning for collecting stem volume information from single trees. ISPRS J. Photogramm. Remote Sens. **123**: 140–158. doi:10.1016/j.isprsjprs.2016.11.012.

Saarinen, N., Kankare, V., Pyörälä, J., Yrttimaa, T., Liang, X., Wulder, M.A., et al. 2019. Assessing the effects of sample size on parametrizing a taper curve equation and the resultant stem-volume estimates. Forests, **10**(10): 848. doi:10.3390/f10100848.

Sabatia, C.O., and Burkhart, H.E. 2015. On the use of upper stem diameters to localize a segmented taper equation to new trees. For. Sci. **61**(3): 411–423. doi:10.5849/forsci.14-039.

Sanquetta, M.N.I., McTague, J.P., Scolforo, H.F., Behling, A., Sanquetta, C.R., and Schmidt, L.N. 2020. What factors should be accounted for when developing a generalized taper function for black wattle trees? Can. J. For. Res. **50**(11): 1113–1123. doi:10.1139/cjfr-2020-0163.

Schneider, R. 2019. Understanding the factors influencing stem form with modelling tools. *In* Progress in botany. Vol. 80. *Edited by* F.M. Cánovas, U. Lüttge, R. Matyssek, and H. Pretzsch. Springer International Publishing, Cham, Switzerland.

Schneider, R., Fortin, M., and Saucier, J.P. 2013. Équations de défilement en forêt naturelle pour les principales essences commerciales du Québec. Mémoire de Recherche Forestière No. 168, Gouvernement du Québec, Ministère des Ressources naturelles, Direction de la recherche forestière. 34pp.

Schneider, R., Franceschini, T., Fortin, M., and Saucier, J.-P. 2018. Climate-induced changes in the stem form of 5 North American tree species. For. Ecol. Manage. **427**: 446–455. doi:10.1016/j.foreco.2017.12.026.

Schumacher, F.X., and Hall, F.S. 1933. Logarithmic expression of timber tree volume. J. Agric. Res. **47**: 719–734.

Scolforo, H.F., McTague, J.P., Raimundo, M.R., Weiskittel, A., Carrero, O., and Scolforo, J.R.S. 2018. Comparison of taper functions applied to eucalypts of varying genetics in Brazil: application and evaluation of the penalized mixed spline approach. Can. J. For. Res. **48**(5): 568–580. doi:10.1139/cjfr-2017-0366.

Shahzad, M.K., Hussain, A., and Jiang, L. 2020. A model form for stem taper and volume estimates of Asian white birch (*Betula platyphylla*): a major commercial tree species of Northeast China. Can. J. For. Res. **50**: 274–286.

Sharma, M. 2020. Incorporating stand density effects in modeling the taper of red pine plantations. Can. J. For. Res. **50**(8): 751–759. doi:10.1139/cjfr-2020-0064.

Sharma, M., and Oderwald, R.G. 2001. Dimensionally compatible volume and taper equations. Can. J. For. Res. **31**(5): 797–803. doi:10.1139/x01-005.

Sharma, M., and Parton, J. 2009. Modeling stand density effects on taper for jack pine and black spruce plantations using dimensional analysis. For. Sci. **55**: 268–282. doi:10.1093/forestscience/55.3.268.

Sharma, M., and Zhang, S. 2004. Variable-exponent taper equations for jack pine, black spruce, and balsam fir in eastern Canada. Can. J. For. Res. **198**: 39–53. doi:10.1016/j.foreco.2004.03.035.

Socha, J., Netzel, P., and Cywicka, D. 2020. Stem taper approximation by artificial neural network and a regression set models. Forests, **11**(1): 79. doi:10.3390/f11010079.

Spurr, S.H. 1952. Forest inventory. Ronald Press, New York. 476pp.

Stängle, S.M., Weiskittel, A.R., Dormann, C.F., and Brüchert, F. 2016. Measurement and prediction of bark thickness in *Picea abies*: assessment of accuracy, precision, and sample size requirements. Can. J. For. Res. **46**(1): 39–47. doi:10.1139/cjfr-2015-0263.

Subedi, N., Sharma, M., and Parton, J. 2011. Effects of sample size and tree selection criteria on the performance of taper equations. Scand. J. For. Res. **26**(6): 555–567. doi:10.1080/02827581.2011.583677.

Sun, Y., Liang, X., Liang, Z., Welham, C., and Li, W. 2016. Deriving merchantable volume in poplar through a localized tapering function from non-destructive terrestrial laser scanning. Forests, **7**(12): 87. doi:10.3390/f7040087.

Tasissa, G., Burkhart, H.E., and Amateis, R.L. 1997. Volume and taper equations for thinned and unthinned loblolly pine trees in cutover, site-prepared plantations. South. J. Appl. For. **21**(3): 146–152. doi:10.1093/sjaf/21.3.146.

Taskhiri, M.S., Hafezi, M.H., Harle, R., Williams, D., Kundu, T., and Turner, P. 2020. Ultrasonic and thermal testing to non-destructively identify internal defects in plantation eucalypts. Comput. Electron. Agric. **173**: 105396. doi:10.1016/j.compag.2020.105396.

Téo, S.J., do Amaral Machado, S., Figueiredo Filho, A., and Tomé, M. 2018. Stem taper equation with extensive applicability to several age classes of *Pinus taeda* L. Floresta, **48**(4): 471–482. doi:10.5380/rf.v48i4.50996.

Thomas, C.E., and Parresol, B.R. 1991. Simple, flexible, trigonometric taper equations. Can. J. For. Res. **21**(7): 1132–1137. doi:10.1139/x91-157.

Trincado, G., and Burkhart, H.E. 2006. A generalized approach for modeling and localizing stem profile curves. For. Sci. **52**: 670–682.

Ung, C.-H., Jing Guo, X., and Fortin, M. 2013. Canadian national taper models. For. Chron. **89**(02): 211–224. doi:10.5558/tfc2013-040.

Valentine, H.T., and Gregoire, T.G. 2001. A switching model of bole taper. Can. J. For. Res. **31**(8): 1400–1409. doi:10.1139/x01-061.

Van Deusen, P.C., Matney, T.G., and Sullivan, A.D. 1982. A compatible system for predicting the volume and diameter of sweetgum trees to any height. South. J. Appl. For. **6**(3): 159–163. doi:10.1093/sjaf/6.3.159.

von Gadow, K., and Hui, G. 1999. Modelling forest development. Kluwer Academic, Dordrecht, the Netherlands. 228pp.

Walsh, C., and Dawson, J.O. 2014. Variation in buttressing form and stem volume ratio of baldcypress trees. Transactions of the Illinois State Academy of Science, 107.

Weiskittel, A., and Li, R. 2012. Development of regional taper and volume equations: Hardwood species. 2011 Annual Report. *Edited by* B. Roth. University of Maine, Cooperative Forestry Research Unit, Orono, Me.

Weiskittel, A.R., Hann, D.W., Kershaw, J.A., Jr., and Vanclay, J.K. 2011. Forest growth and yield modeling. John Wiley & Sons, Chichester, U.K.

Weiskittel, A., Radtke, P., Westfall, J., Walker, D., Affleck, D., Coulston, J., and MacFarlane, D.W. 2020. National Scale Biomass Estimator (NSBE) project: next steps, implications, and future timeline. *In* Celebrating progress, possibilities, and partnerships: Proceedings of the 2019 Forest Inventory and Analysis (FIA) Science Stakeholder Meeting, 19–21 November 2019, Knoxville, Tenn. USDA For. Serv. e–Gen. Tech. Rep. SRS–256. *Edited by* T.J. Brandeis. US Department of Agriculture, Forest Service, Southern Research Station, Asheville, N.C. pp. 73–74.

Wensel, L.C., and Olson, C.M. 1995. Tree volume equations for major California conifers. Hilgardia, **62**(2): 1–73. doi:10.3733/hilg.v62n02p014.

Westfall, J.A., and Scott, C.T. 2010. Taper models for commercial tree species in the Northeastern United States. For. Sci. **56**: 515–528.

Westfall, J.A., McRoberts, R.E., Radtke, P.J., and Weiskittel, A.R. 2016. Effects of uncertainty in upper-stem diameter information on tree volume estimates. Eur. J. For. Res. **135**(5): 937–947. doi:10.1007/s10342-016-0985-4.

Yang, S.-I., and Burkhart, H.E. 2020. Robustness of parametric and nonparametric fitting procedures of tree-stem taper with alternative definitions for validation data. J. For. **118**: 576–583. doi:10.1093/jofore/fvaa036.

Yang, Y., Huang, S., Trincado, G., and Meng, S.X. 2009. Nonlinear mixed-effects modeling of variable-exponent taper equations for lodgepole pine in Alberta, Canada. Eur. J. For. Res. **128**(4): 415–429. doi:10.1007/s10342-009-0286-2.

Zakrzewski, W.T. 1999. A mathematically tractable stem profile model for jack pine in Ontario. North. J. Appl. For. **16**(3): 138–143. doi:10.1093/njaf/16.3.138.

Zakrzewski, W.T. 2009. Defining tree taper: A challenge for growth and yield modelling in Ontario. For. Chron. **85**(6): 897–899. doi:10.5558/tfc85897-6.

Zakrzewski, W.T., and MacFarlane, D.W. 2006. Regional stem profile model for cross-border comparisons of harvested red pine (*Pinus resinosa* Ait.) in Ontario and Michigan. For. Sci. **52**: 468–475. doi:10.1093/forestscience/52.4.468.

Zhao, D., Lynch, T.B., Westfall, J., Coulston, J., Kane, M., and Adams, D.E. 2019. Compatibility, development, and estimation of taper and volume equation systems. For. Sci. **65**(1): 1–13. doi:10.1093/forsci/fxy036.